POWER DEMAND REDUCTION IN ELECTRIC VEHICLE CHARGING

A PROJECT REPORT

submitted by

NOWFAL S

TKM21EEPS09

to

the APJ Abdul Kalam Technological University

in partial fulfillment of the requirements for the award of the

Degree

of

Master of Technology

in

Power Systems

DEPARTMENT OF ELECTRICAL AND ELECTRONICS ENGINEERING

T.K.M. COLLEGE OF ENGINEERING, KOLLAM

APRIL-MAY, 2023

DEPARTMENT OF ELECTRICAL AND ELECTRONICS ENGINEERING.

T.K.M COLLEGE OF ENGINEERING, KOLLAM

CERTIFICATE

This is to certify that the report entitled **'POWER DEMAND REDUCTION IN ELECTRIC VEHICLE CHARGING'** submitted by **NOWFAL S** to the APJ Abdul Kalam Technological University in partial fulfillment of the requirements for the award of the Degree of Master of Technology in Electrical and Electronics Engineering is a bonafide record of the project work carried out by him under our guidance and supervision. This project report in any form has not been submitted to any other University or Institute for any purpose.

Prof. Shanavas T N
Internal Supervisor
Associate Professor
Dept of EEE, TKMCE

(External Examiner)

Prof. Jibi P Mathew
Project Coordinator
Asst. Professor
Dept of EEE, TKMCE

Dr. Sabeena Beevi K
Head of Department
Professor
Dept of EEE, TKMCE

ACKNOWLEDGEMENT

First of all I am indebted to the **God Almighty** for giving me an opportunity to excel in my effort to complete this project on time.

I am extremely grateful to **Dr. T. Shahul Hameed**, Principal, TKM College of Engineering, and **Dr. Sabeena Beevi. K**, Head of the Department, Department of Electrical and Electronics Engineering, for providing all required resources for the successful completion of my project.

I am greatly obliged to **Prof. Shanavas T. N.** , Associate Professor, PG co-ordinator, Department of Electrical and Electronics Engineering, for his encouragement and support.

My heartfelt gratitude to **Prof. Shanavas T. N.** , Associate Professor, Project Guide, Department of Electrical and Electronics Engineering, for his valuable suggestions and guidance in the preparation of the project report.

I express my thanks to **Prof. Jibi P Mathew**, Asst. Professor, Project co-ordinator, Department of Electrical and Electronics Engineering, and all staff members and friends for all help and co-ordination extended in bringing out this project successfully in time.

I will be failing in duty if I do not acknowledge with grateful thanks to the authors of the references and other literature referred to in this project.

Last, but not least, I am very much thankful to my parents who guided me in every step which I took.

Place: Kollam NOWFAL S

Date: APRIL-MAY, 2023 TKM21EEPS09

ABSTRACT

Due to rising fossil fuel prices and accelerating carbon dioxide (CO2) emissions, the use of electric vehicles (EVs) has grown over the past few years. At present EV charging stations use the existing utility power grid, and hence there is an increase in load demand at the distribution side and thereby stress on the utility grid. There are different solutions for this problem, mainly PV integration, Power factor correction (PFC) in chargers, managed charging, indirect power demand reduction, etc. For a level 1 EV charging, AC to DC conversion and also its power factor correction is necessary. There are multiple problems with the diode bridge rectifier used in typical chargers, notably conduction loss and nonlinear characteristics. Bridge rectifiers with input diodes operate poorly, are inefficient, and also have a low power factor. This project focuses on important EV power demand reduction strategies like PFC, charging with on-site renewable energy, and indirect power demand reduction. This project make use of a novel Cuk-SEPIC converter with fuzzy logic control for PFC and calculating its power factor.This topology is compared with two other converter topologies (Cuk-push-pull, and Cuk-flyback). All these converters are designed to work in discontinuous conduction mode. The Cuk-SEPIC converter is the integration of both Cuk and SEPIC converters in which the Cuk converter works in the positive half and the SEPIC converter works in the negative half cycle. The next objective is the integration of PV in level 2 charging along with its design, cost analysis, and simulations for reducing power demand on the grid

Contents

List of Figures

List of Tables

Abbreviations and Notations

1. DBR: Diode Bridge Rectifier
2. PFC: Power Factor Correction
3. DCM: Discontinuous Conduction Mode
4. CCM: Continuous Conduction Mode
5. BL: Bridgeless
6. SEPIC: Single-Ended Primary-Inductor Converter
7. PV: Photo Voltaic
8. EV: Electric Vehicle
9. MPP: Maximum PowerPoint
10. MPPT: Maximum Power Point Tracking
11. P&O: Perturbation and observation
12. FLC: Fuzzy Logic Controller

Chapter 1

Introduction

1.1 General Background

Without a doubt, the most popular and reasonably priced method of transportation for people worldwide is by road. But, the environmental problems and high dependency on fossil create a huge problem. Due to this, the market for electric vehicles has expanded, and EV acceptance has dramatically increased globally. Consequently, EVs are the way of the future, and EV technology is advancing quickly every day. India wants to become more sustainable and reduce its carbon footprint, so the government is constantly adopting transportation reforms that aim to electrify all practical modes of transportation.

The graph in Figure 1.1 shows the number of EV sales from 2019 to 2021. It is clear from this data that the number of EVs is growing quickly. According to the stated policies, an emerging nation like India would have roughly 50% electric automobiles by the year 2030. Due to their lesser dependence on fossil fuels and lower pollution, electric vehicles are growing in popularity. EVs come in a variety of forms, including hybrid, plug-in hybrid, plug-in EV, etc. Plug-in EVs are entirely powered by a sizable battery pack, which is charged by an external power source via a plug. Both the Onboard and off-board battery chargers of EVs can have a

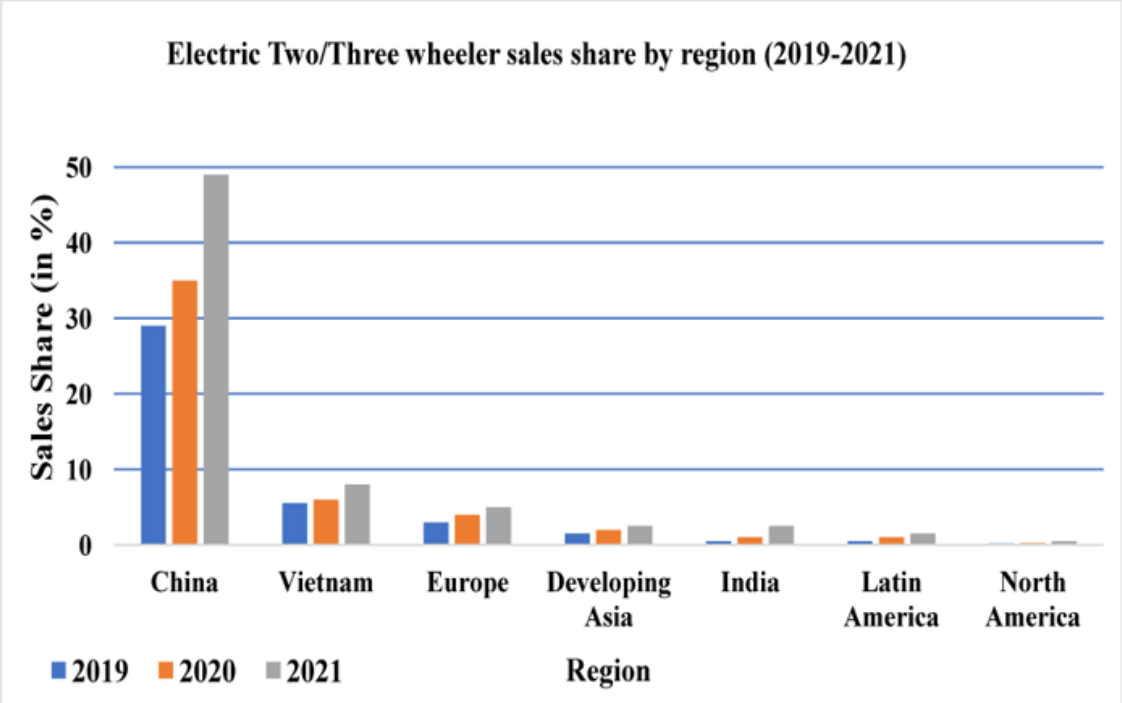

Fig. 1.1: EV sales

unidirectional or bidirectional power flow. A bidirectional charging system provides sufficient power, by grid and battery integration. onboard chargers provide an extra burden to EVs than offboard chargers in case of weight, space, and price limits. Systems for onboard charging can be either inductive or conductive. In the conductive charging system, the connector is connected to the charging inlet directly. In inductive charging, the power is transferred indirectly which means without any medium for example magnetic or wireless transfer. For this type of charging the vehicle needs not to be stationary. There are three charging levels when it comes to EVs: level 1, level 2, and level 3. While level 3 is quick charging, level 1 is the slower charging that is often used at home. Level 2 charging is commonly used in private or public while level 3 is used in commercial such as gas stations. Different charge levels are shown in Fig 1.2. Onboard chargers are typically used at levels 1 and 2, and off-board chargers (rapid charging) are used at level 3.

1.2 Motivation

The number of EVs is rising in a rapid speed, but one of the crucial consid-

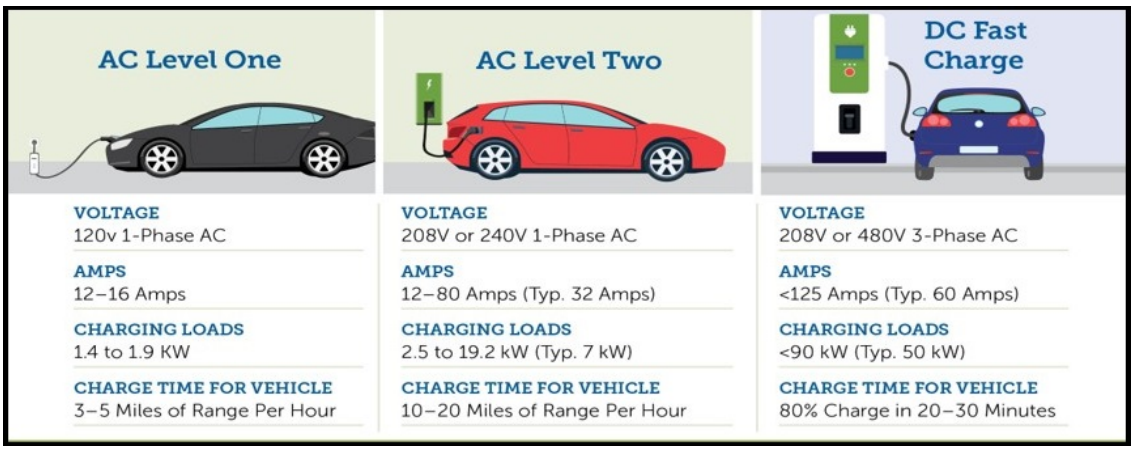

Fig. 1.2: Charging levels

erations is how much this will cost the grid. Just consider what would happen if all all-electric vehicles were linked to the grid for charging at the same time. Huge electricity consumption will result from it. India's projected EV electricity demand by 2030 is expected to be 69.6 TWh. Due to the high demand for electricity, there are numerous issues, including power network clustering, outages, load shedding, power shortages, electricity bill rise, and pollution. There are different solutions for this power demand problem such as Managed Charging(it's charging accordingly, for example Arranging the time of charging according to the peak demand), Using alternative energy sources to reduce the dependency on the grid supply, EVs can also act as an energy storage device by giving supply to the grid in the time of shortfalls, network Charging, charging with on-site renewables, PFC in chargers, indirect power demand reduction, discounts for Times of Peak Renewable Energy Availability, etc.

1.3 Thesis objectives

This project focuses on important EV power demand reduction strategies like PFC, charging with on-site renewable energy, and indirect power demand reduction. This project primarily focuses on introducing a novel Cuk-SEPIC converter with fuzzy logic control for PFC, calculating its power factor, and comparing it to two other converter topologies (Cuk-push pull and Cuk-flyback). The next objective is the integration of PV in level 2 charging along with its design, cost, and simulations

for reducing power demand. Fig.1.3 shows the complete objective of this project.

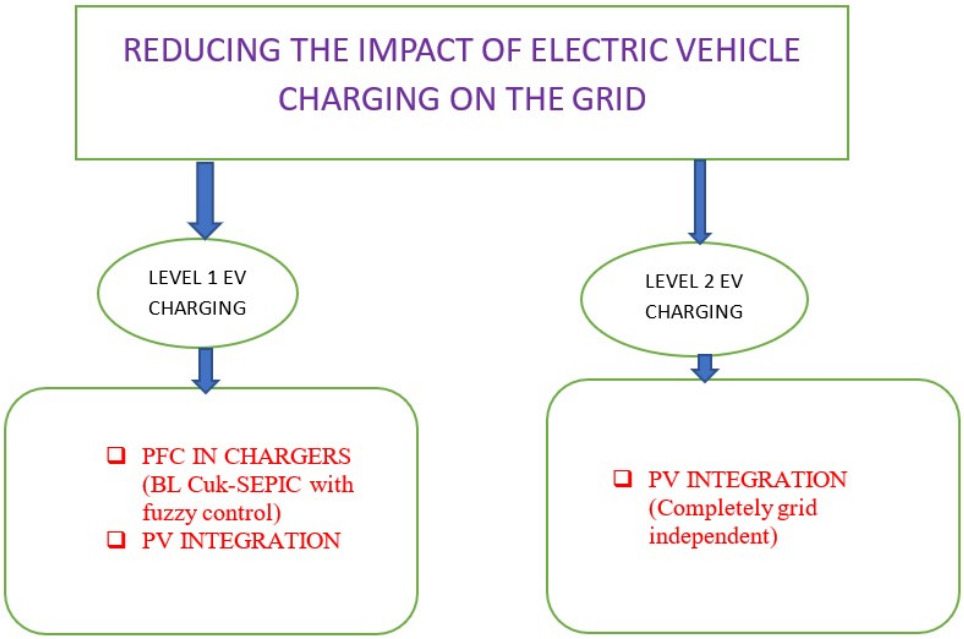

Fig. 1.3: Power demand reduction techniques

Chapter 2

Literature Survey

2.1 Introduction

This chapter provides a detailed description of the previous works which have been done on similar topics.

2.2 An Improved Battery Charger for Electric Vehicle with High Power Factor

The buck-boost arrangement is used in this study to explore a simpler bridgeless topology for EV battery chargers, which significantly minimizes conduction loss by reducing the number of components. In order to control the charging of a 48V/100Ah battery across a constant current (CC)/constant voltage (CV) profile and to inherit built-in PFC capabilities at the side of the main, a flyback converter is presented in this paper. Here, the author presents a bridgeless (BL) buck-boost converter which is non isolated for input power factor adjustment of an EV battery charger that feeds a flyback converter made to make it easier to charge an EV battery in constant current and constant voltage mode. Using voltage follower mode control, the proposed topology here operates two series-connected buck-boost converters in positive and negative half-line cycles to maintain a constant intermediate

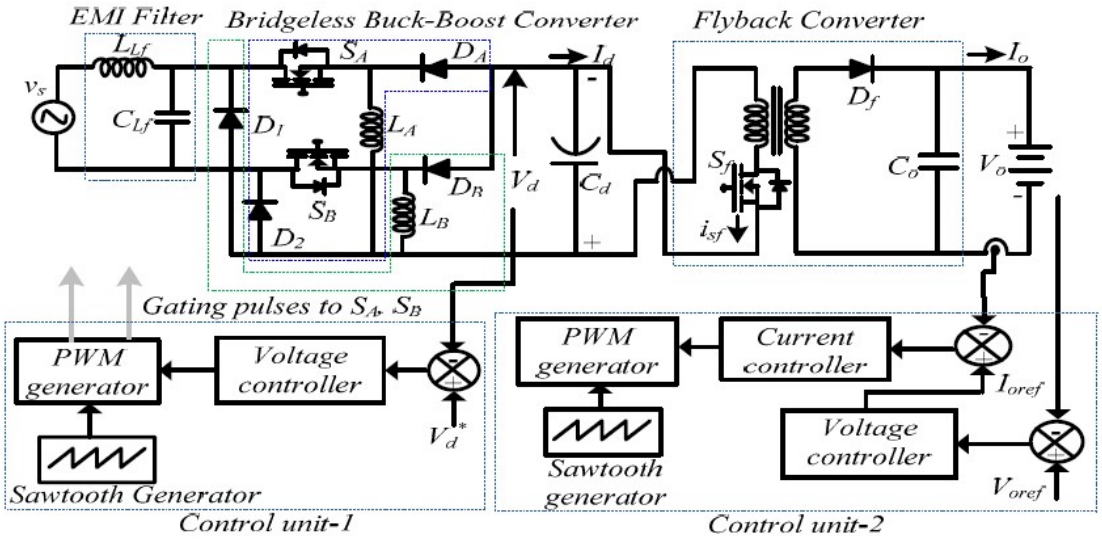

Fig. 2.1: BL Buck-Boost converter with Fly-back DC-DC Converter

DC link voltage. For the flyback converter to be fed at the output, the PFC converter can withstand a broad range in mains voltage. Using a dual PI controller, the proposed charger operation is managed in DCM mode. Additionally, the charger's input current is modified to operate at UPF while having a low input harmonic content.

2.3 New Efficient Bridgeless Cuk Rectifiers for PFC Applications

This study discusses three innovative Cuk topological bridgeless single-phase ac-dc power factor correction (PFC) rectifiers.The main practical shortcomings of the bridgeless boost rectifier are identical to those of traditional boost converters, including the fact that the dc output voltage is higher than the peak input voltage, the absence of galvanic isolation, and the large start-up inrush currents. In order to step down the voltage, an extra converter or an isolation transformer is needed for low-output voltage applications such as those in the telecommunication or computer industries.The Cuk converter has a number of benefits in PFC applications, including simple transformer isolation implementation, inherent protection against

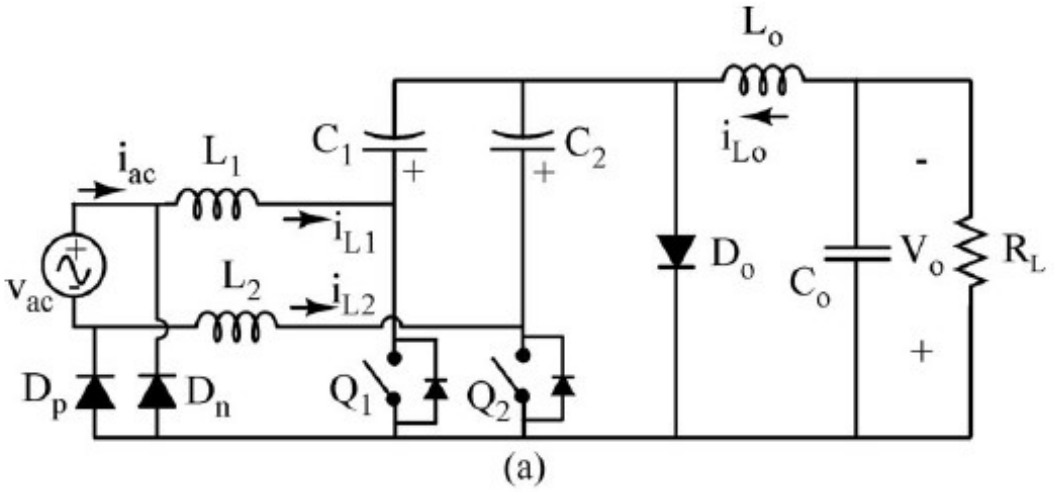

Fig. 2.2: BL Cuk Topology.1.

start-up or overload current inrushes, lower input current ripple, and reduced electromagnetic interference (EMI) brought on by the DCM topology. When compared to a conventional Cuk PFC rectifier, this one has better thermal management due to the absence of an input diode bridge and the use of just two semiconductor switches in the current flow path during each interval of the switching cycle. The suggested topologies in this paper are designed to operate in DCM to obtain nearly a unity power factor and little input current total harmonic distortion. Additional benefits of the DCM operation include zero-current power switch turn-on, zero-current output diode turn-off, and simple control circuitry. Fig. 2.2,2.3,2.4 depicts the three bridgeless Cuk PFC rectifiers that are suggested in this paper. Here, two dc-dc Cuk converters are connected, one for each half-line period of the input voltage, to create the suggested topologies. The two power switches (Q1 and Q2) are used in the proposed bridgeless rectifiers. However, the control circuitry can be greatly simplified by driving both power switches with the same control signal. The structure of the proposed topologies uses one more inductor than the traditional Cuk topology, which is frequently cited as a drawback in terms of size, EMI and cost. However, compared to a single inductor, the two inductors can produce a better thermal performance.The current conduction path for type 2 has the fewest semiconductor components. The floating switch and a step-up voltage gain of more than two, however, are two drawbacks. The floating switch requires a more com-

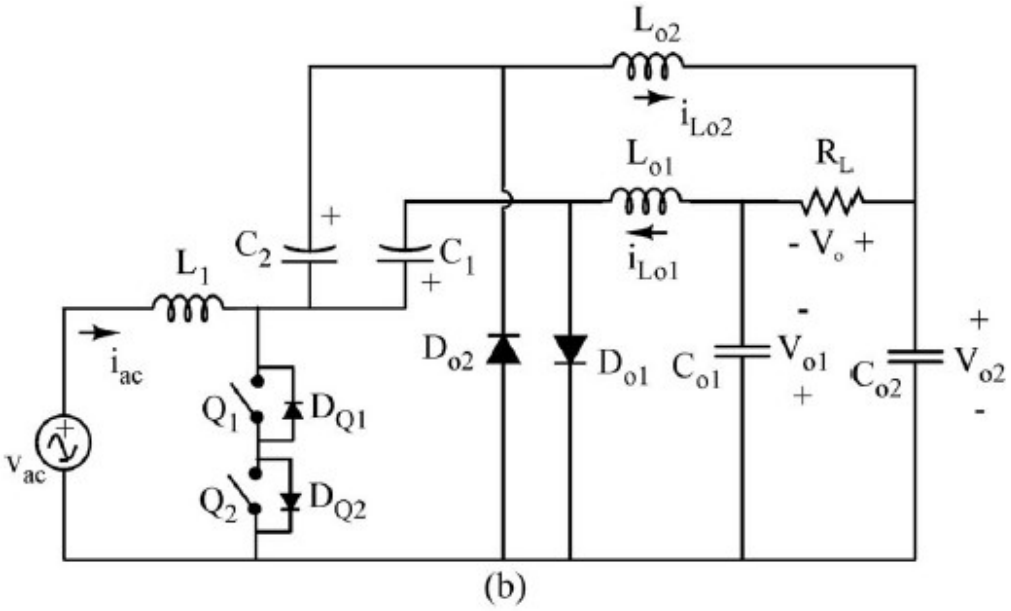

Fig. 2.3: BL Cuk Topology.2.

plex driver circuitry and frequently generates higher electromagnetic emissions.The advantage of Type 1 is that it has fewer components overall but a greater current peak. Type 3 has fewer pressures but a greater component count. In summary, the converter of choice depends on the application. When compared to the traditional Cuk PFC rectifier, the topologies proposed here can further increase conversion efficiency because they have lower conduction and switching losses. In particular, the proposed circuits can operate at a higher switching frequency while yet maintaining the same efficiency. As a result, the size of the EMI filter and PFC inductor might be further reduced. Comparing the proposed bridgeless topologies in this paper to the traditional PFC Cuk rectifier, efficiency can be increased by about 1.4%.

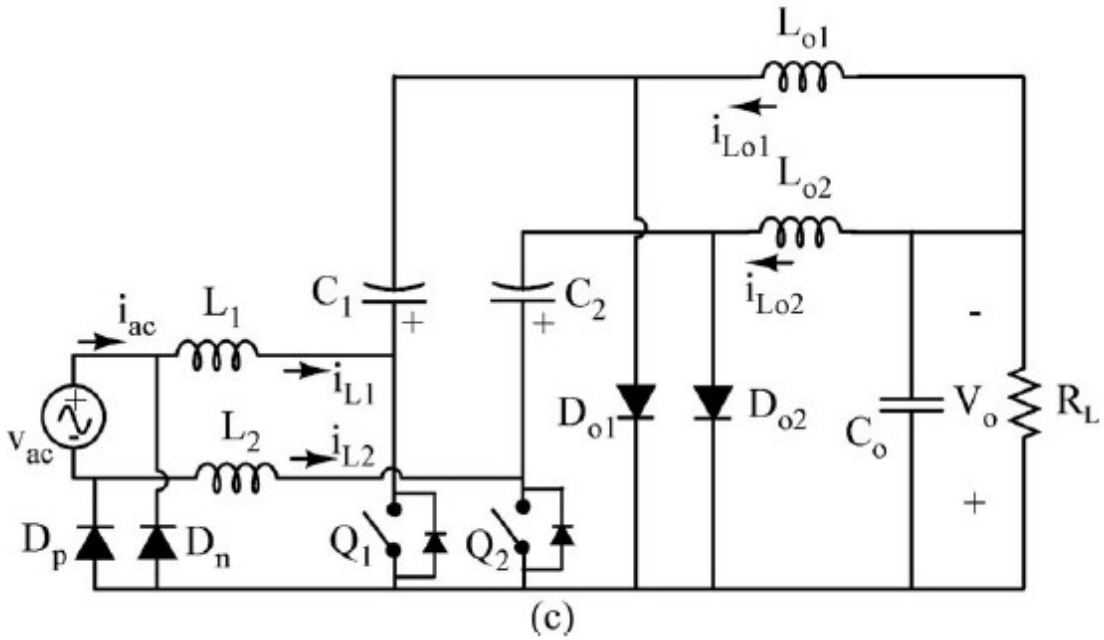

Fig. 2.4: BL Cuk Topology.3.

2.4 A PFC Based EV Battery Charger Using a Bridgeless Isolated SEPIC Converter

Another type of converter that can offer a better power factor is the BL SEPIC converter. There are fewer components compared to the Cuk topology. In the SEPIC topology, there is only one input inductor.The working is similar in both the half cycle. During the positive half cycle, switch S_1 is triggered, and as a result of that, the magnetizing inductance L_{m1} and diode D_1 come into action. During the negative half cycle, switch S_1 becomes turned off and S_2 is triggered. This makes diode D_2 and magnetizing inductance L_{m2} come into conduction. At the end of each switching cycle, the current in the magnetic inductance of the high-frequency transformer becomes discontinuous (DCM) There are three modes of operation for each half cycle. These modes are similar in both positive and negative half cycles due to similar waveforms. A dual loop controller is utilized with the suggested charger to ensure the best possible charging of the EV battery. There are two switches that function in synchronism for the positive and negative half cycles of each half of the input supply voltage. The control circuitry uses a voltage PI controller to pre-regulate the battery voltage, V_{dc}, in order to charge an EV battery utilizing a

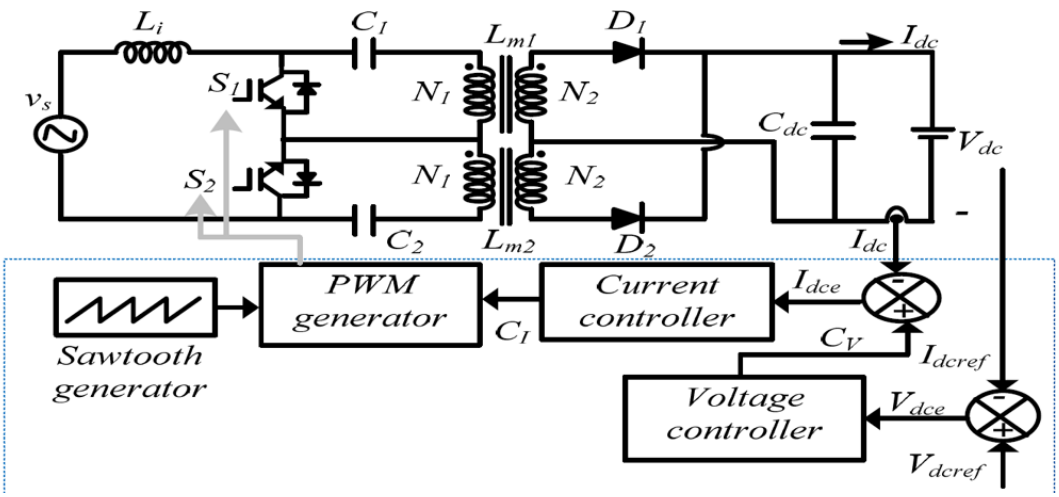

Fig. 2.5: BL SEPIC converter topology

constant current/constant voltage technique. Here two PI controllers are used for the battery control. one PI for the outer loop and one for the inner loop. The outer loop is voltage control while the inner loop is current control.

A 760W, BL isolated SEPIC converter can be designed from the below equations. Here the supply voltage is considered as 220V and the output voltage as 65V.

Average supply voltage,

$$V_{av} = \frac{2\sqrt{2}V_s}{3.14} \tag{2.1}$$

V_s is the input voltage, D is the duty cycle and N1/N2 is the transformation ratio.

$$V_{dc} = \frac{N_2 V_{av} D}{N_1(1-D)} \tag{2.2}$$

where V_{dc} is the output voltage. Δi_i is the input ripple current of the input inductor, here it's determined in order to offer CCM across one switching period.

$$L_i = \frac{V_s \times D}{\Delta i_i \times 2f_s} \tag{2.3}$$

where f_s is the switching frequency. The critical magnetizing inductance value

is determined as follows,

$$L_{mc} = \frac{(n^2)V_{dc}(1-D)^2}{2Df_sI_{dc}} \tag{2.4}$$

The chosen magnetizing inductance value must be less than the calculated critical magnetizing value to provide DCM operation.

$$C_{1,2} = \frac{N_2V_{dc} \times D}{N_1\Delta V_{c1,2} \times f_sR_{dc}} \tag{2.5}$$

From the above equation, the intermediate capacitor voltage can be calculated. The DC link capacitor to supply rated battery load, is estimated as,

$$C_{dc} = \frac{I_{dc}}{2\omega\Delta V_{dc}} \tag{2.6}$$

2.5 Review of Battery Charger Topologies, Charging Power Levels, and Infrastructure for Plug-In Electric and Hybrid Vehicles

This paper analyses the infrastructure for plug-in electric vehicles and hybrids, as well as the present state of battery chargers, charging power levels, and implementation. Off-board and on-board charger types with unidirectional or bidirectional power flow are divided into different categories. Unidirectional charging reduces the amount of hardware needed and makes connecting problems easier. Battery energy injection back into the grid is supported by bidirectional charging. Due to weight, space, and price restrictions, typical onboard chargers have power limitations. To prevent these issues, they can be combined with the electric drive. The need for and expense of onboard energy storage is reduced by the presence of charging infrastructure. Systems for onboard charging can be either inductive or conductive. An off-board charger has fewer size and weight restrictions and can be made to charge at high speeds. There is a discussion of Level 1 (convenient), Level 2 (main), and Level 3 (rapid) power levels. It presents future elements like charging for roadbeds. The amount of power, charging time and location, cost, equipment,

and other variables are presented, contrasted, and evaluated for various power-level chargers and infrastructure configurations.

Battery performance is influenced by charger parameters and charging infrastructure in addition to the battery type and design. There are three different types of battery infrastructure and charging power: Level 1, Level 2, and Level 3. Off-board and on-board types of charger systems with unidirectional and bidirectional power flow are divided into these categories. Unidirectional charging reduces the amount of hardware needed, makes interconnection problems easier, and slows down battery deterioration. Battery energy injection back into the grid is supported by bidirectional charging. Common onboard chargers have power limitations to adhere to weight, space, and price restrictions. By utilizing the electric drive system as an integrated charger, these issues may be prevented. The main benefit of integrated chargers is that they offer bidirectional fast charging with a unity power factor at a cheap cost and high power (Levels 2 and 3). The requirement, as well as the expense of onboard energy storage, are reduced by the presence of charging infrastructure. Systems for onboard charging can be either inductive or conductive. Active roadbed systems could eventually be supported by inductive charging. Several teams are researching these. On the basis of the amount of power, charging time and location, cost, suitability, equipment required, and other variables, different charger power levels, and infrastructure designs were presented in this paper and analyzed. Standardization of guidelines and infrastructure choices, effective and intelligent chargers, and improved battery technologies are all necessary for EV success.

Chapter 3

Power factor Correction in EV charger

PFC is one of the most important sections of an EV charger, especially for level 1 charging, or residential charging. It prevents additional strain on the grid during charging. The EV charging mechanism is shown in Fig.3.1. The existence

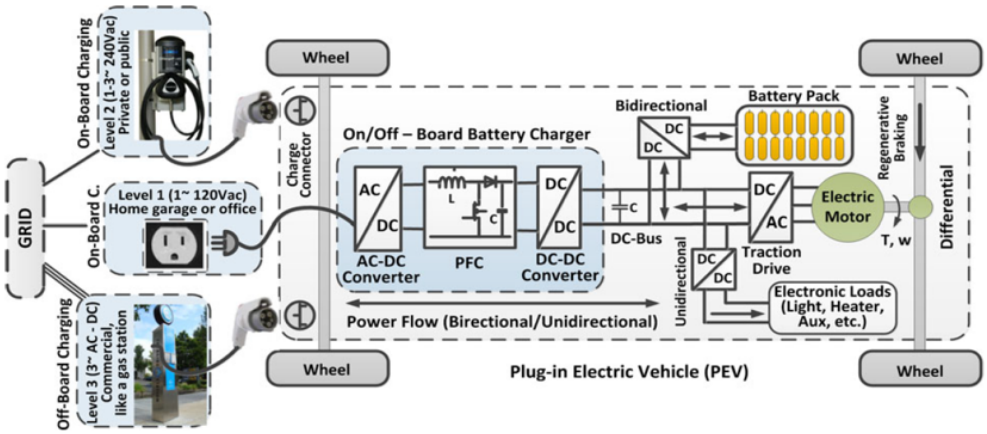

Fig. 3.1: Charging system

of a diode bridge at the input side of a conventional rectifier causes numerous issues, and the power factor is one of them. As a result, this section considers converter topologies without bridges, also known as bridgeless converter topologies. An AC-DC converter, which is essentially a rectifier, is used in the level 1 charger to give

single-phase ac power to the battery. The input power factor (PF) is worsened by the traditional diode bridge rectifier (DBR)-based EV charger, which also has total harmonic distortion (THD) that can reach as high as 55.3%. Power factor correction is required for an AC to DC conversion. The diode bridge rectifier used in conventional chargers has a number of issues, most notably conduction loss and nonlinear properties. In addition to operating badly and being inefficient, bridge rectifiers with input diodes also have poor current shaping capabilities, duty cycle restrictions, etc. Other converter topologies can be utilized to get around these problems. Buck and boost converters are not encouraged for PF correction in chargers due to their poor wave-shaping capabilities and constrained duty cycle. When interleaved PFC converters are taken into account, the charger becomes bulkier due to issues like high current stress and heat dissipation. Therefore, in this project, we will first analyze various converter topologies, such as the Cuk-flyback converter topology and the Cuk-push pull converter topology.

3.1 BL Cuk Converter

One of the better converter topologies for power factor correction is the BL Cuk converter. Fig.3.2 depicts the cuk topology, in which the output is connected to a battery through a dc-dc converter and the input is an ac source. Here, a dc-dc converter could be a push-pull, flyback, etc. This DC-DC converter aids in giving the battery a suitable input. The input of Cuk is single-phase ac, while the Cuk is made up of two switches, an intermediate capacitor, two output inductors, an input inductor, and a dc link. It is intended for the converter to operate in DCM mode. The Cuk converter completes the circuit like, $L_{i1} - S_1 - D_{o1} - L_{o1} - D_p$, in the positive half cycle. In the negative half cycle, the circuit completes like this, $L_{i2} - S_2 - D_{o2} - L_{o2} - D_n$. Both the Cuk converter input inductors L_{i1} and L_{i2} are designed to operate in CCM. However, it is certain by the design of output inductors L_{o1} and L_{o2} that the converter enters DCM within one switching cycle and the output diode current, i_D, is zero. The intermediate capacitors C_1 and C_2 are chosen so that the voltage across the capacitors is continuous throughout the

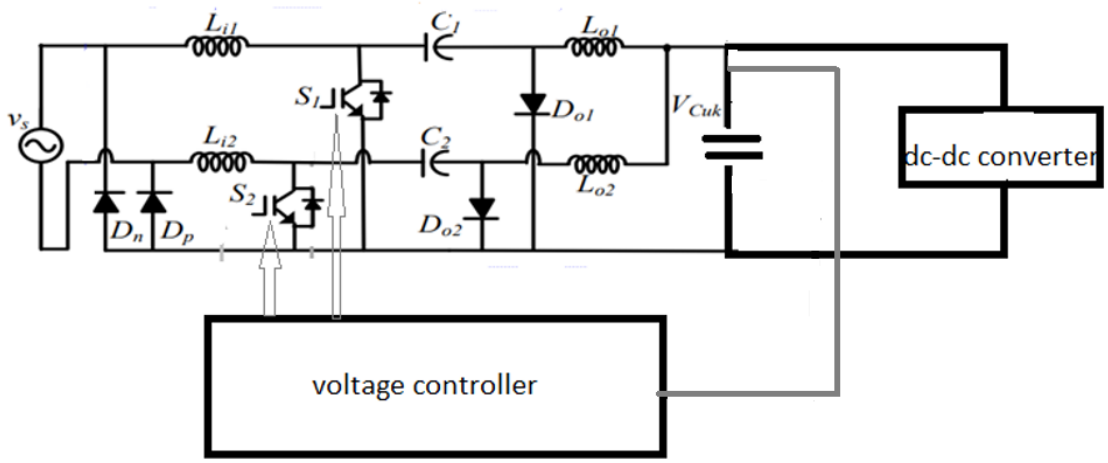

Fig. 3.2: BL Cuk converter topology

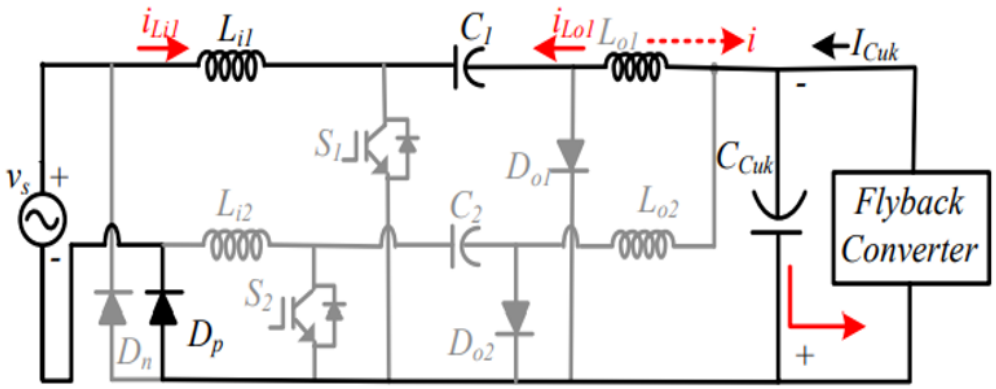

Fig. 3.3: Cuk DCM mode

whole switching period. At the end of the switching period converter enters into a mode called DCM where both the inductors completely discharge the stored energy and the net current through the output side diode becomes zero(Fig.3.3). It is important to note that the same PWM signal is used to drive both switches S_1 and S_2, which lowers the system cost and circuit complexity. Single-loop voltage feedback control is utilized to maintain the output voltage of the Cuk converter, which lowers the cost of the charger because only one voltage sensor is required. Here the cuk is made to produce 300V of output from a 220V input. From equation 3.1, the duty cycle can be calculated where M is the gain and K_e is the dimensionless parameter taken as 0.08 for this application.

$$D_{Cuk} = \sqrt{2}M\sqrt{2}K_e \tag{3.1}$$

The net inductance, L_{eq} can be found from the below equation where f_s is the switching frequency which is taken as 20KHz.

$$L_{eq} = \frac{k_e R_{Cuk}}{2f_s} \tag{3.2}$$

The input inductance, $L_{i1,2}$ can be found from the below equation where Δi is the peak ripple current value which is taken as 40% of the input inductor current.

$$L_{i1,2} = \frac{V_{in}D}{\Delta i f_s} \tag{3.3}$$

From net and input inductance, the output inductance $L_{01,2}$ can be calculated.

$$L_{01,2} = \frac{L_{eq}L_{i1,2}}{L_{eq} - L_{i1,2}} \tag{3.4}$$

The intermediate capacitor value can be calculated from the below equation where the resonant frequency is taken as 1.5KHz.

$$C_{1,2} = \frac{1}{\omega^2(L_{i1,2} + L_{01,2})} \tag{3.5}$$

$$C_{Cuk} = \frac{I_{Cuk}}{2\omega\Delta V_{Cuk}} \tag{3.6}$$

C_{Cuk} is the dc link capacitor value, which can be found from the above equation where Δv_{Cuk} is the output voltage ripple value which is taken as 1% of the output Cuk voltage. With the above equations, the Cuk parameter values can be calculated and shown in Table 3.1. The flyback converter duty cycle D_f can be calculated from the below equation,

$$\frac{V_{Cuk}}{N} + V_{batt} = \frac{V_{batt}}{D_f} \tag{3.7}$$

Where N is the flyback transformation ratio. The value of the critical magnetizing inductance can be calculated from equation 3.8 and the value selected should be

less than the calculated value to ensure DCM.

$$L_m = \frac{(V_{Cuk} D_f)^2}{2 V_{batt} I_{batt} f_{sf}} \tag{3.8}$$

The outer capacitor voltage can be calculated from the below equation, here the capacitor voltage ripple is considered as 0.1% of output voltage and f_{sf} is the switching frequency of the flyback converter.

$$C_o = \frac{V_{batt} D_f}{\frac{(V_{batt})^2}{P} \gamma V_{batt} f_{sf}} \tag{3.9}$$

The parameter value of the push-pull converter can also be calculated using the above equations. The flyback and push-pull parameter values are shown in Tables 3.2 and 3.3.

Table 3.1: Cuk Converter parameters

PARAMETER OF CUK CONVERTER	**PARAMETER VALUES**
Input Inductor	4mH
Duty Cycle	0.384
Switching Frequency	20kHZ
Intermediate Capacitor	3μF
DC link	1.5mH
Output Inductor	150μH

Table 3.2: flyback Converter parameters

PARAMETER OF flyback CONVERTER	**PARAMETER VALUES**
Transformation ratio	3
Duty Cycle	0.394
Switching Frequency	50kHZ
Magnetizing inductance	130μH
Outer capacitor	2mF

Table 3.3: Push-pull Converter parameters

PARAMETER OF Push-pull CONVERTER	**PARAMETER VALUES**
Transformation ratio	3
Duty Cycle	0.394
Switching Frequency	50kHZ
Magnetizing inductance	2.79 mH
Outer capacitor	2mF

3.2 Cuk-SEPIC Converter with fuzzy controller

The Cuk converter topology can offer a better PFC, but because it's a multi-stage design, it also has several drawbacks, including low efficiency and conduction loss. The output inductor current of a SEPIC is discontinuous, which might shorten a battery's lifespan. So here proposing a new converter topology by integrating Cuk and SEPIC called Cuk-SEPIC topology with fuzzy control that can provide a flexible duty cycle. The BL Cuk-SEPIC converter is designed to work in DCM mode in order to provide a unity power factor and also to provide a wide range of duty cycles. The Cuk-SEPIC converter is obtained by integrating cuk and sepic together in which Cuk act in the positive half cycle and SEPIC act in the negative half cycle. In the positive half cycle, the switch S_1, intermediate capacitor C_1, HFT magnetizing inductance L_{m1}, and output diode D_{o1} conducts. In the negative half cycle, the switch S_2, intermediate capacitor C_2, HFT magnetizing inductance L_{m2}, and output diode D_{o2} conducts.

3.2.1 Design of a Cuk-SEPIC converter

The design procedure of a BL Cuk-SEPIC EV chargers are given below. The output voltage of the BL Cuk-SEPIC converter is need to be maintained constant nearly at 65V. The input voltage here consider is 220V and the peak value is 311V.

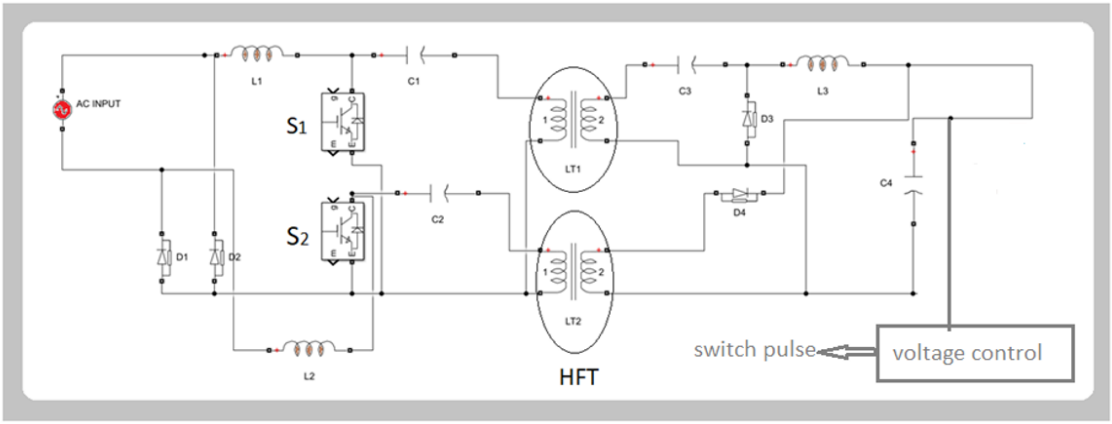

Fig. 3.4: Proposed Cuk-sepic topology

$$V_{dc} = \frac{N_2 D}{N_1(1-D)} V_{in} \tag{3.10}$$

where N2/N1 is the transformation ratio, which is considered as 0.5 for this application. So from the above equation, the duty cycle can be obtained which is 0.29. There is a critical value for the HFT and it can be obtained from equation 3.8.

$$L_{m1,2} = \frac{V_{in} D}{2 I_{in} f_s} = 295.07\mu H(100\mu H, DCM) \tag{3.11}$$

where fs is the switching frequency, which is taken as 20 kHz.In order to work the converter in DCM, the magnetizing inductance value should be less than the magnetizing critical value. So here it's taken as 100 μH. The value of both the input inductors can be get from the below equation,

$$L_{1,2} = \frac{V_{in} D}{\Delta i f_s} = 2.95mH(3mH) \tag{3.12}$$

Here the input ripple current is taken as 20% of the input current., Here the value obtained is 2.95 mH and it's taken as 3 mH for this application. Intermediate capacitor C1,2 is calculated as,

$$C_{1,2} = \frac{V_{in} n^2 D^2}{\Delta c_{1,2} R f_s (1-D)} = 1.03\mu F(1\mu F) \tag{3.13}$$

Δ $c_{1,2}$ is the capacitor voltage ripple which is considered as 20% of the input

capacitor voltage. Here the obtained value is 1.03μF. A value of 1μ F is taken to work it in continuous conduction for the entire switching cycle. The value of capacitor C_3 can be found from,

$$C_3 = \frac{V_{dc}D}{\Delta V_{c3}Rf_s} = 11.74\mu F(12\mu F) \tag{3.14}$$

ΔV_{C3} is the ripple voltage which is taken as 20% of the output voltage, The capacitance C_3 is selected as 12 μF . The output inductance L_o can be calculated from the below equation,

$$L_0 = \frac{V_{dc}(1-D)}{\Delta I_{L0}f_s} = 795.85\mu H(800\mu H) \tag{3.15}$$

Here the ripple current is taken as 20% of the output current. The output inductor value is taken as 800μH. The required dc-link capacitor is calculated from,

$$C_{dc} = \frac{I_{dc}}{2\omega\Delta V_{dc}} = 9.79mF(10mF) \tag{3.16}$$

Here ΔV_{dc} is the ripple voltage which is considered as 3% of the output voltage. The value of ω is 2πf where f is the resonant frequency which is taken as 1.5kHZ. Here the dc link capacitor taken is 10 mF.

Table 3.4: Cuk-SEPIC Converter parameters

PARAMETER OF Cuk-SEPIC CONVERTER	**PARAMETER VALUES**
Turns ratio	0.5
Duty Cycle	0.29
Switching Frequency	20kHZ
Magnetizing inductance	100μH
Input inductors	3mH
Intermediate capacitor	1μF
Output side capacitor(C_3)	12μF
Output inductor	800μH
DC Link capacitor	10mF

3.2.2 Fuzzy Logic Controller

Fuzzy logic, also known as fuzzy set theory, was developed in 1965 by Lotfi Zadeh, a computer scientist at the University of California, Berkeley, as a way to describe and manipulate data that is fuzzier or undefined rather than certain. The professional world first rebuked him, but over time, fuzzy logic (FL) attracted their interest and evolved into a wholly original field of artificial intelligence. The FL is an interesting area of study because it does a fantastic job of preserving precision and meaning, two things that humans have valued for a very long time. A collec-

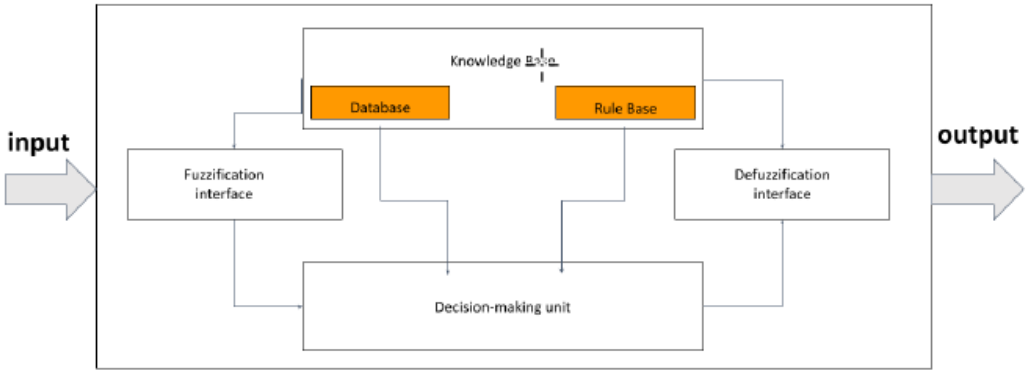

Fig. 3.5: Fuzzy inference system

tion of values that specify the proper approach to control a system is the knowledge that is included in the rule base. Information evaluation has been done using objective functions. The assumption step establishes which current standard solutions were valid, and the plant outputs that must be allowed are then specified. The signals are modified by the fuzzification software so they can be represented when both of the directive's requirements are met. The defuzzification interface converts the inferences made using either plant sources or an inference process. The controller's first component, fuzzification, receives input data and turns it into degrees of membership functions. The fuzzy reference is the second component of the fuzzy controller and contains the knowledge base and decision-making guidelines. It is a procedure to create a mapping from an input to an output using predetermined decision-making criteria.

The voltage control of the Cuk-SEPIC converter is done here using fuzzy control. The output voltage is sensed, compared with a reference signal, and the resulting

error signal is provided to the PI controller if the PI controller is used. A signal is generated and supplied to the PWM generator to produce the pulse for the switches at specific K_P and K_i values. Instead of a PI controller, a fuzzy controller is utilized because it can improve the converter system's control behavior under load and parameter fluctuations, allowing for greater flexibility. For a fuzzy control, simply there are three sections which are input, rule base, and output .In this case, there are 2 inputs,7 membership functions, and an output which is given to generate the pulse. Error(E) and change in error are the two inputs. A memory block can be used to identify the change in error input from the error that results from comparing the reference voltage with the output voltage. These two inputs are given to the fuzzy system and assign a 7membership function for each input and also the output. The 7 membership functions are NS, NM, NB, ZE, PS, PM, and PB. These membership functions create the rule base, which in turn provides the duty ratio. The rule base is shown in Table 3.6. For every combination of membership values

ERROR / CHANGE IN ERROR	NB	NM	NS	ZE	PS	PM	PB
NB	PB	PB	PB	PB	PM	PS	ZE
NM	PB	PB	PB	PM	PS	ZE	NS
NS	PB	PB	PM	PS	ZE	NS	NM
ZE	PB	PM	ZE	NS	NM	NB	NM
PS	PM	PS	ZE	NS	NM	NB	NB
PM	NS	ZE	NS	NM	NB	NB	NB
PB	ZE	NS	NM	NB	NB	NB	NB

Table. 3.6: Rule base

of input has its corresponding output membership value. So, the fuzzy controller provides the duty according to the corresponding input and it's given to a pulse width modulator. The pulse width modulator produces the pulses and the pulses are given to both the switches.

3.3 Simulation

3.3.1 Introduction

The Cuk-SEPIC converter is simulated using MATLAB-Simulink. MATLAB (an abbreviation of "MATrix LABoratory") is a proprietary multi-paradigm programming language and numeric computing environment developed by MathWorks. Matrix manipulation, function and data visualization, algorithm implementation, user interface building, and linking with other programming languages are all possible with MATLAB.

MATLAB is primarily designed for numeric computation, but an optional toolbox that uses the MuPAD symbolic engine gives users access to symbolic computation capabilities. Simulink, a separate program, includes model-based design and graphical multi-domain simulation for dynamic and embedded systems.

3.3.2 Simulation and result

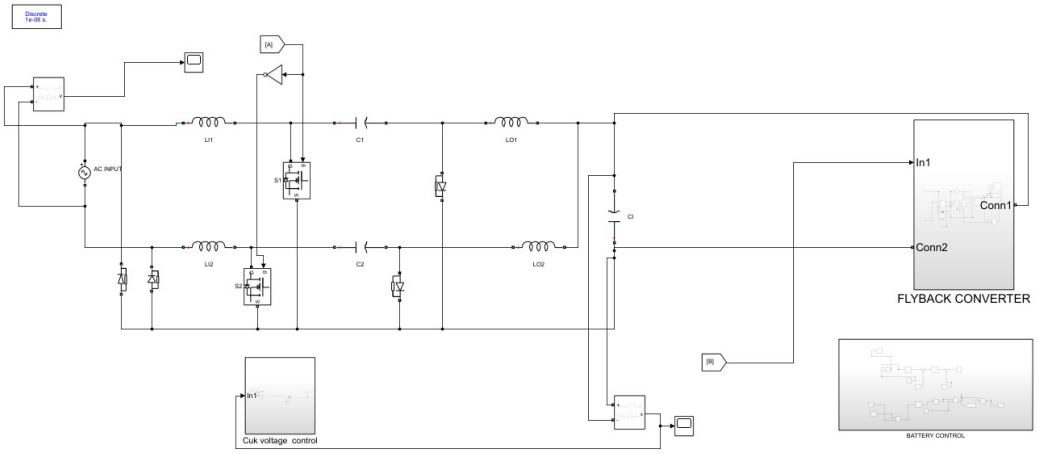

Fig. 3.7: Cuk with flyback converter

The simulation of the Cuk-push pull and Cuk-flyback topologies is shown in Figures 3.7 and 3.8. Using a PI controller with specific kp and ki values, the Cuk output voltage in both converter cases is kept at 300V. When utilizing a Cuk-flyback, the power factor is 0.89, whereas when using a Cuk-push pull, it is 0.95. Both have a higher power factor than the conventional rectifier, which is 0.82. Fig

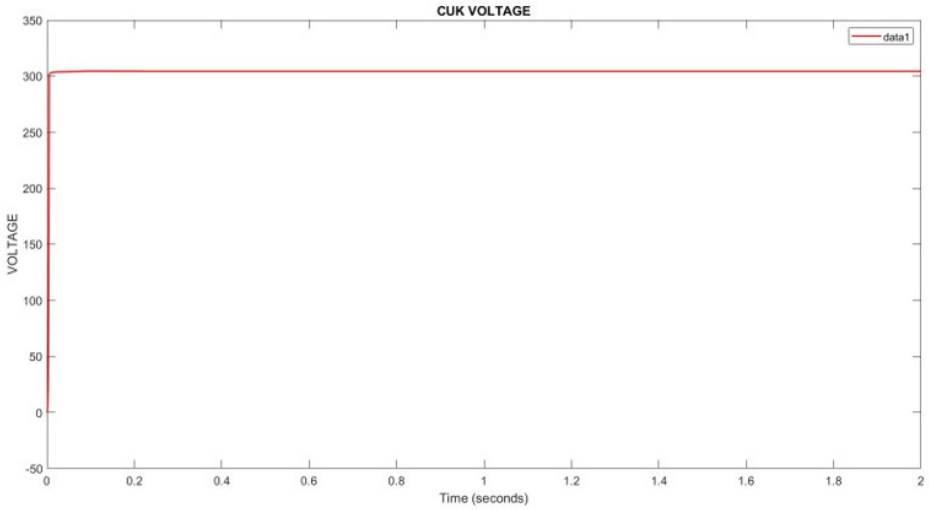

Fig. 3.8: Cuk output voltage

3.12 and 3.13 shows the positive and negative half-cycle simulation of the Cuk-SEPIC converter in which it acts as a Cuk in the positive half and SEPIC on the other half. The output voltage in both cases is around 60V. While the output current in a SEPIC is discontinuous, it is continuous in a cuk. Fig 3.16 is the simulation of the Cuk-SEPIC converter using fuzzy logic control. Here the input voltage given is a peak voltage of 220V which is 311V. Fig.3.18 depicts the input inductor current, which is continuous and has a peak-to-peak current of 4 A. The two switch current is around 28A, which is less than the permitted level of 30A. As shown in Fig.3.23, the primary magnetizing inductance current is obtained. The magnetizing inductance value that defines the period of the DCM mode, and the secondary magnetizing inductance current is discontinuous as intended shown in Fig. 3.24. The value of magnetizing inductance determines the duration of discontinuous mode, here we designed the converter in DCM and a discontinuous peak current of 8A is obtained. Here, the output is kept at 65 volts so it can provide the load. Next, a load is introduced here the load is a battery. A 48V 100Ah battery is connected to the output of the Cuk-SEPIC converter with 80% SOC. The voltage across the battery is 52V which is shown in Fig. 3.26. The SOC during the charging of the battery is shown in Fig.3.28. The battery current is seen to be a continuous current of nearly 12A. The battery current contains a small

peak ripple current(0.15-0.2A) which is less than the allowed value. So it provides smooth charging and long life to the battery. The most important is that the power factor obtained is 0.997, almost nearly one. So it can avoid the extra power demand on the grid in level 1 charging.

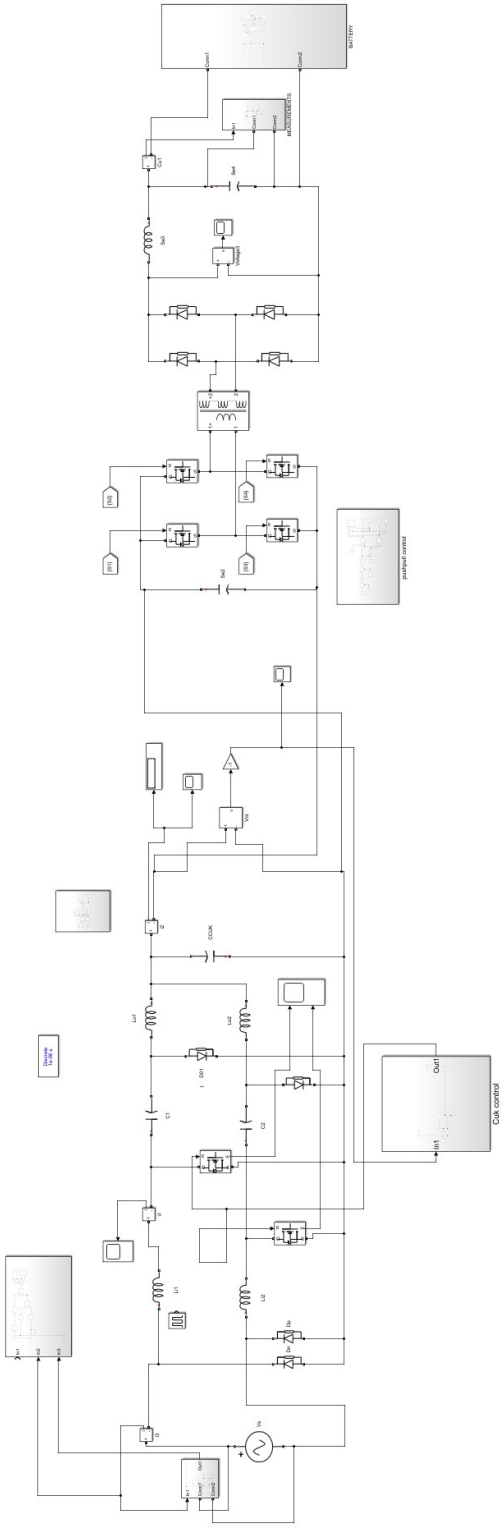

Fig. 3.9: Cuk with push-pull converter

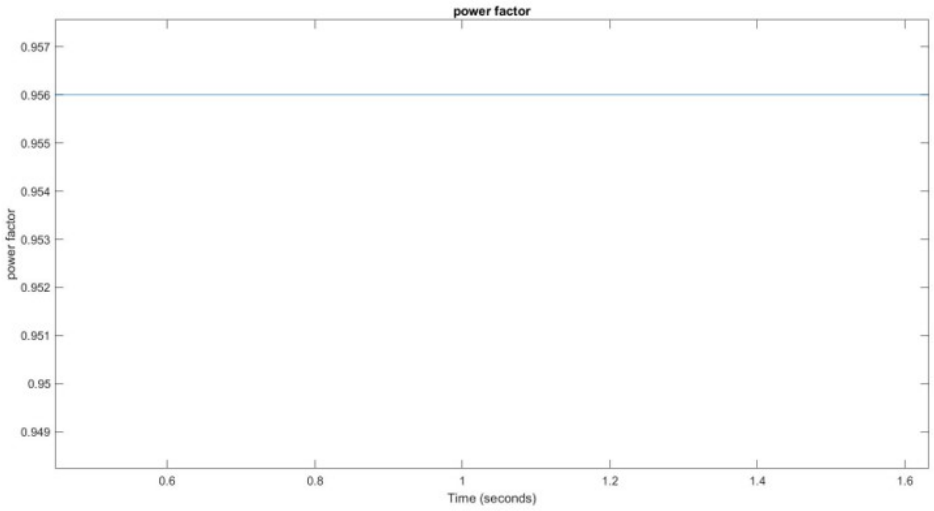

Fig. 3.10: Power factor of Cuk push-pull

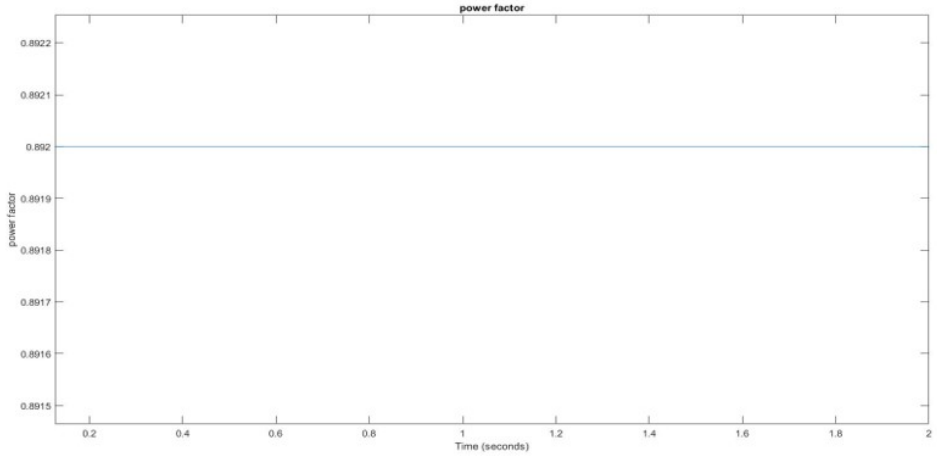

Fig. 3.11: Powerfactor of Cuk-flyback

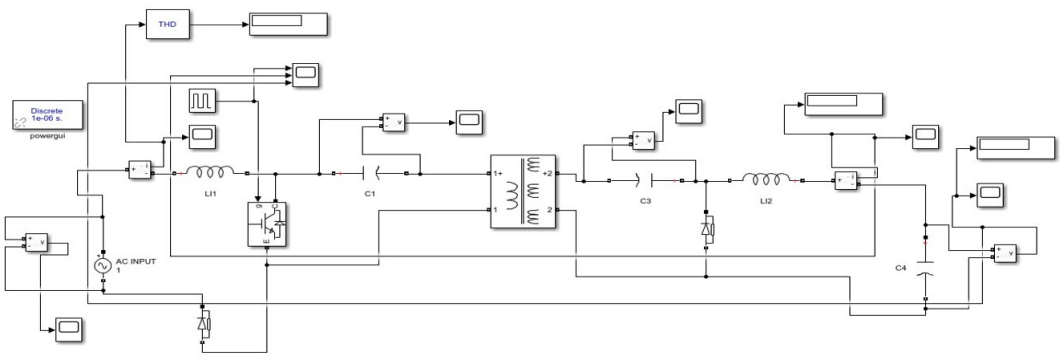

Fig. 3.12: Positive half cycle simulation of Cuk-SEPIC

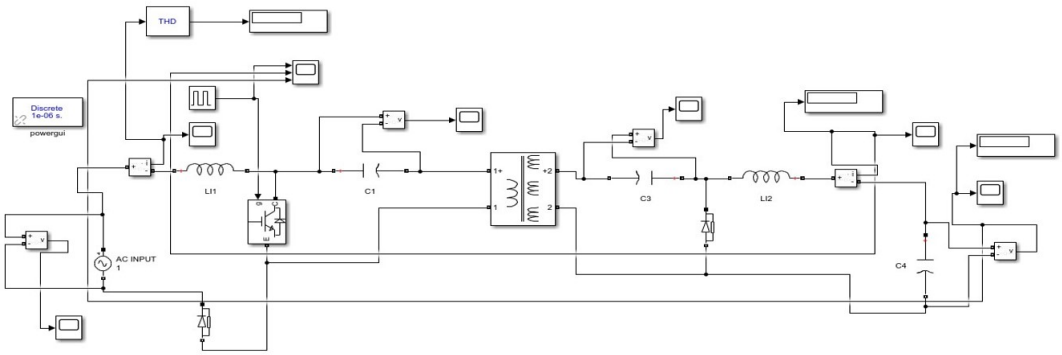

Fig. 3.13: Negative half cycle simulation of Cuk-SEPIC

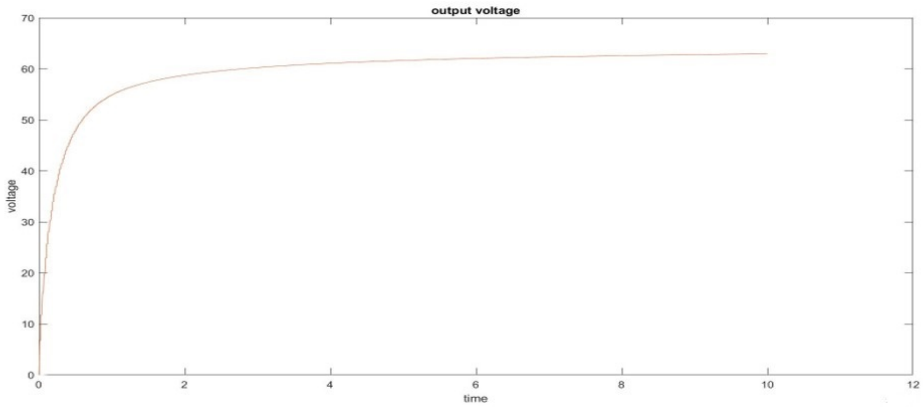

Fig. 3.14: Output voltage in each half of Cuk-SEPIC

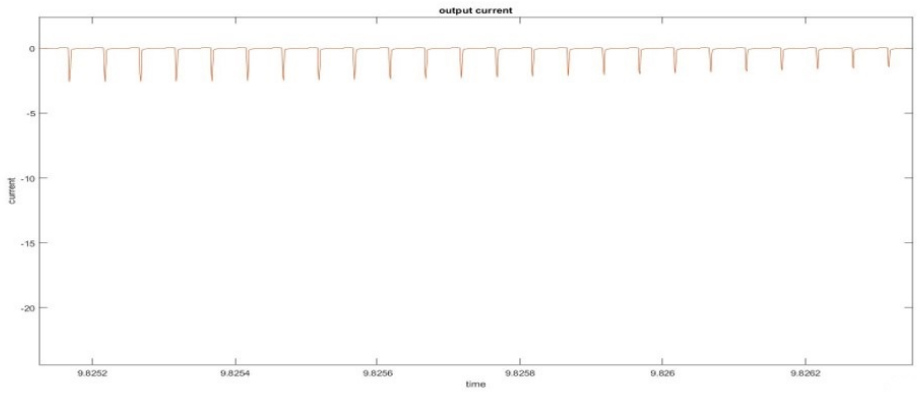

Fig. 3.15: SEPIC output current(negative half)

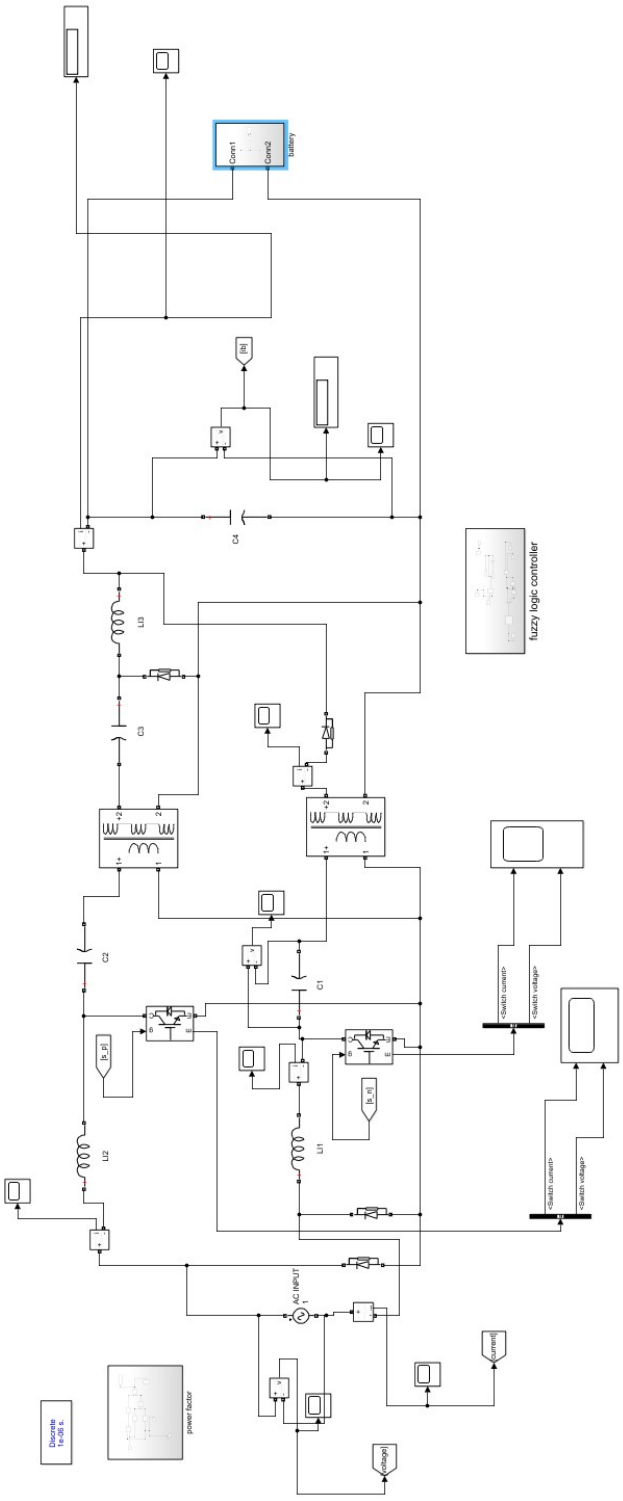

Fig. 3.16: Cuk-SEPIC with fuzzy control

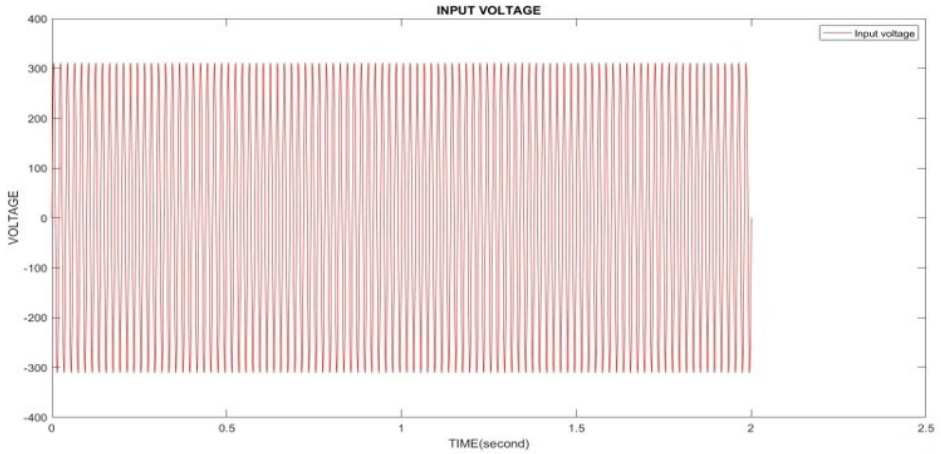

Fig. 3.17: Input voltage

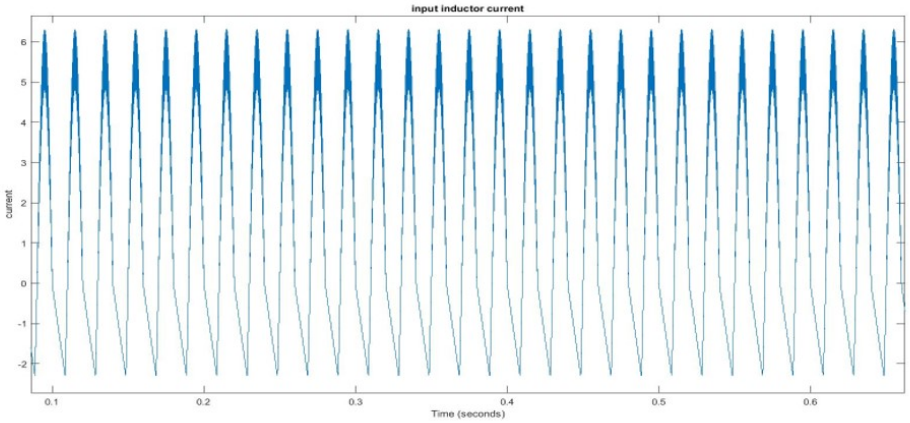

Fig. 3.18: Input inductor current of Cuk-SEPIC

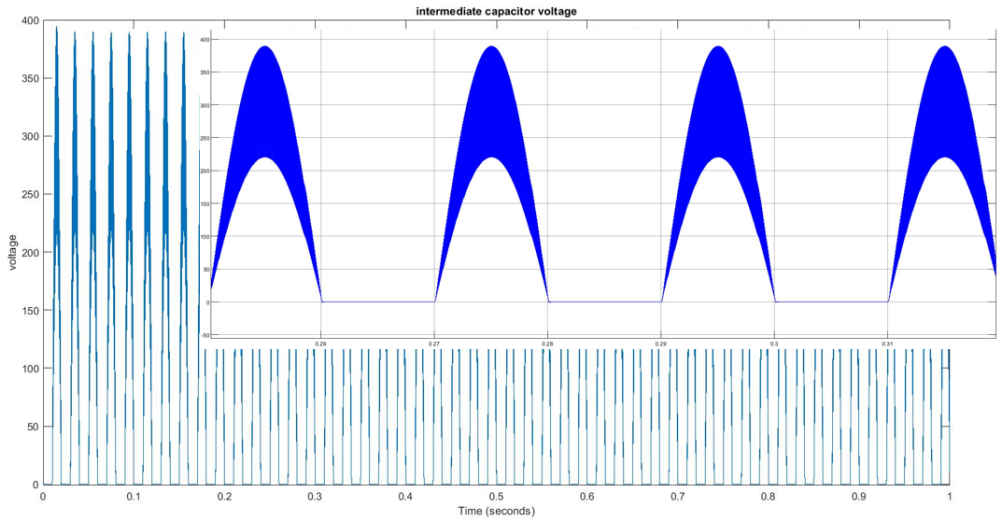

Fig. 3.19: Input capacitor voltage of Cuk-SEPIC

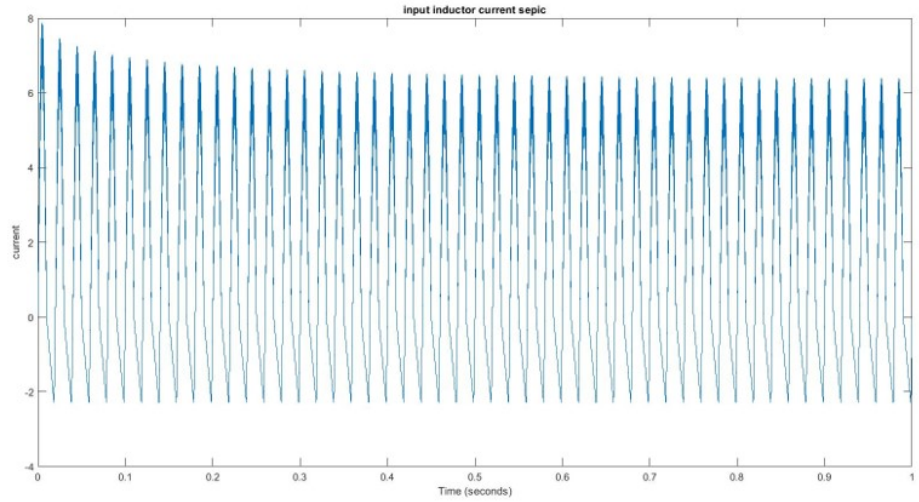

Fig. 3.20: Second input inductor current of Cuk-SEPIC

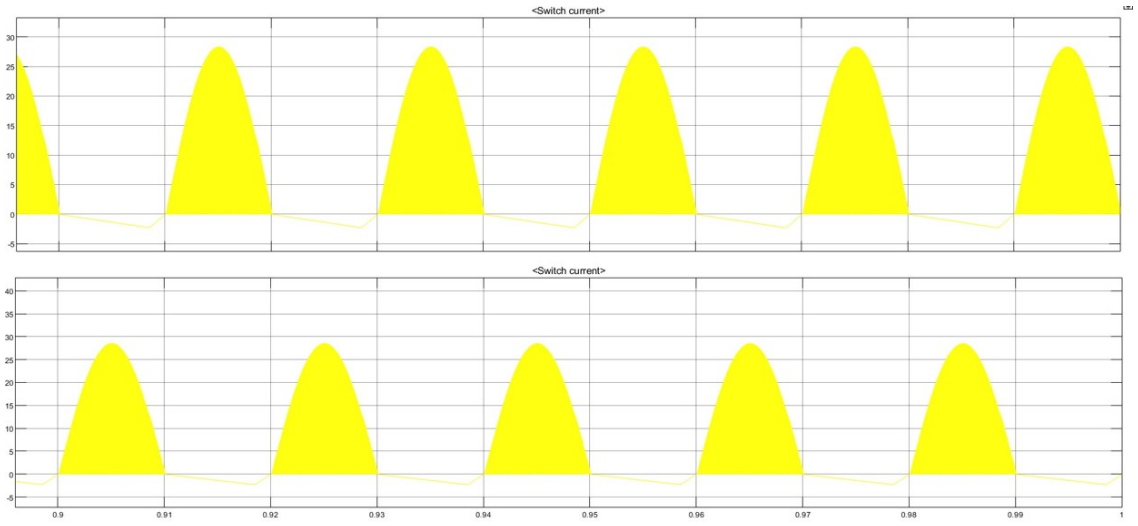

Fig. 3.21: Switch current

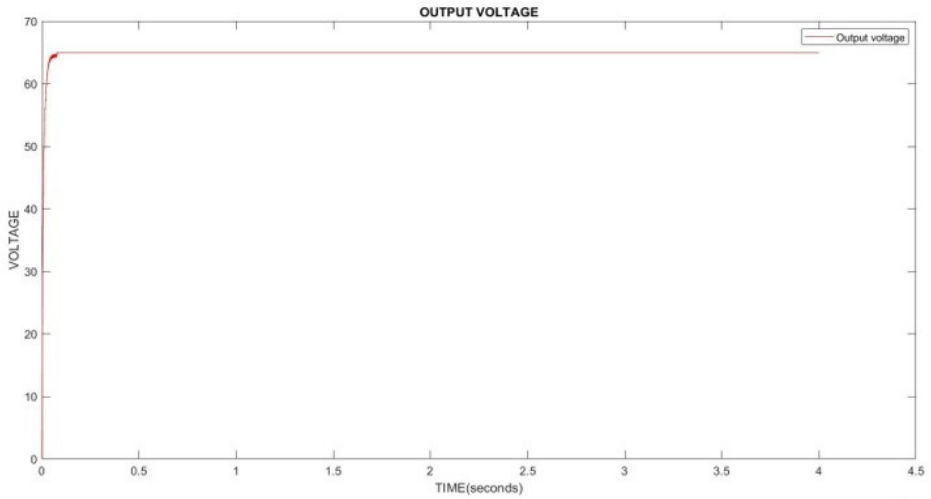

Fig. 3.22: Output voltage of Cuk-SEPIC with fuzzy control

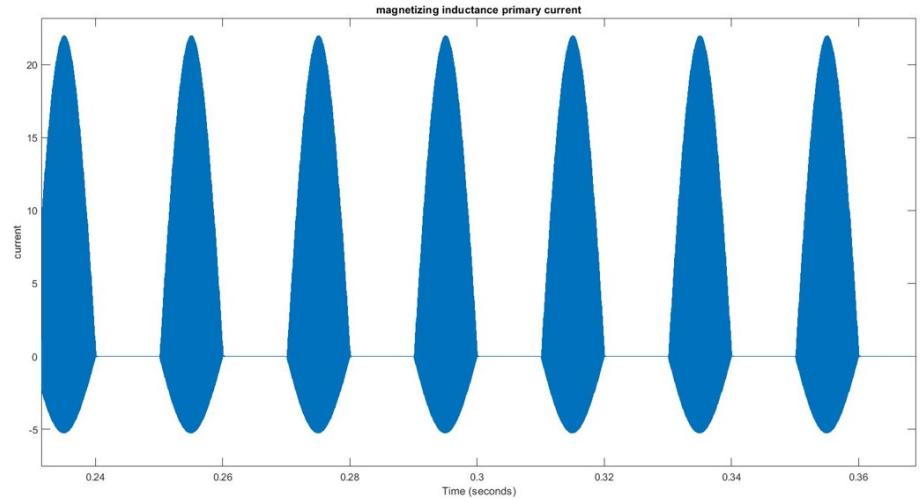

Fig. 3.23: Primary magnetizing inductance current of Cuk-SEPIC

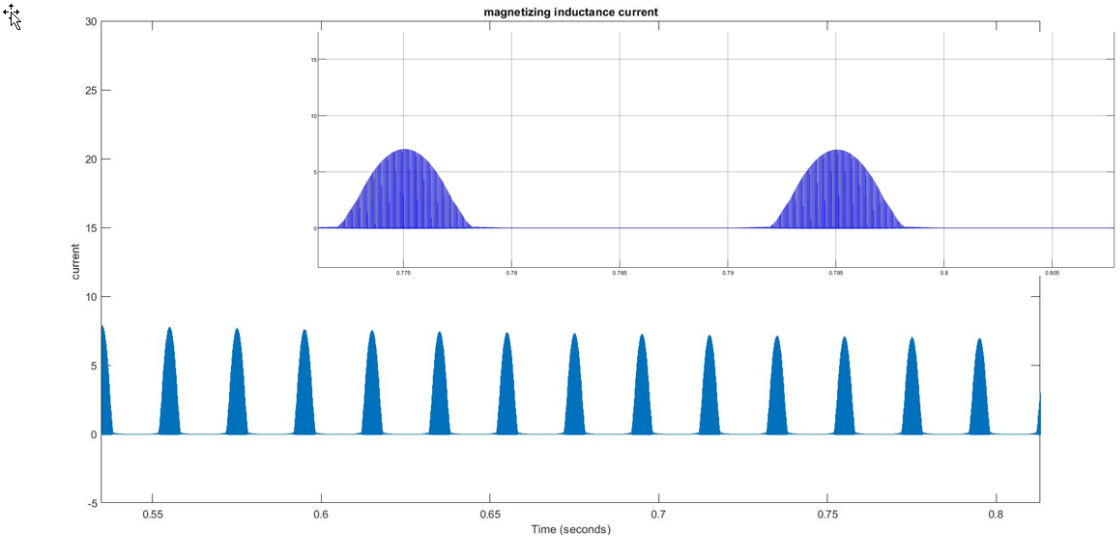

Fig. 3.24: Secondary magnetizing inductance current of Cuk-SEPIC

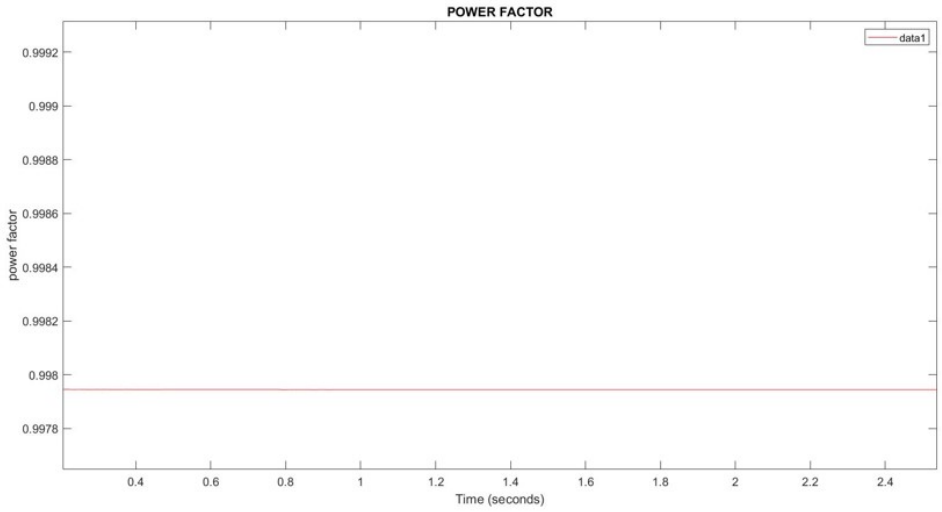

Fig. 3.25: Cuk-SEPIC power factor

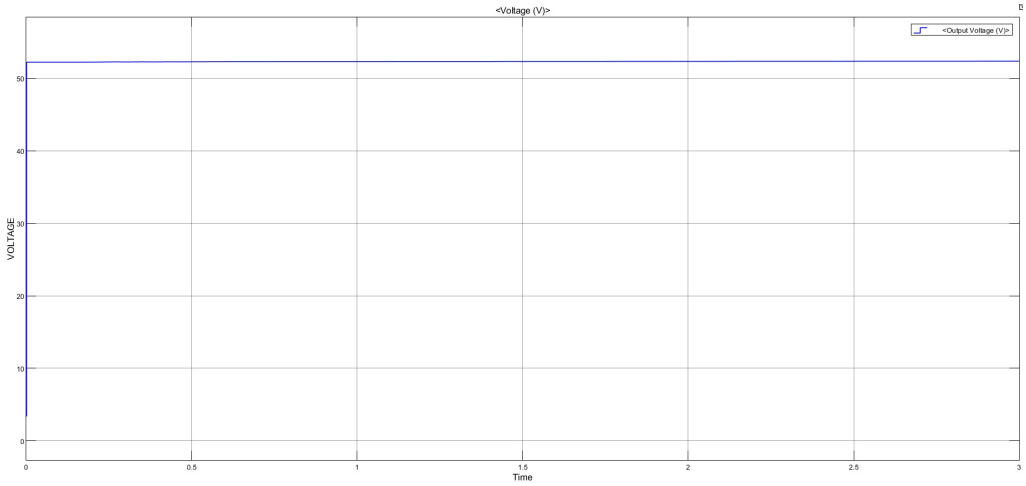

Fig. 3.26: Battery voltage

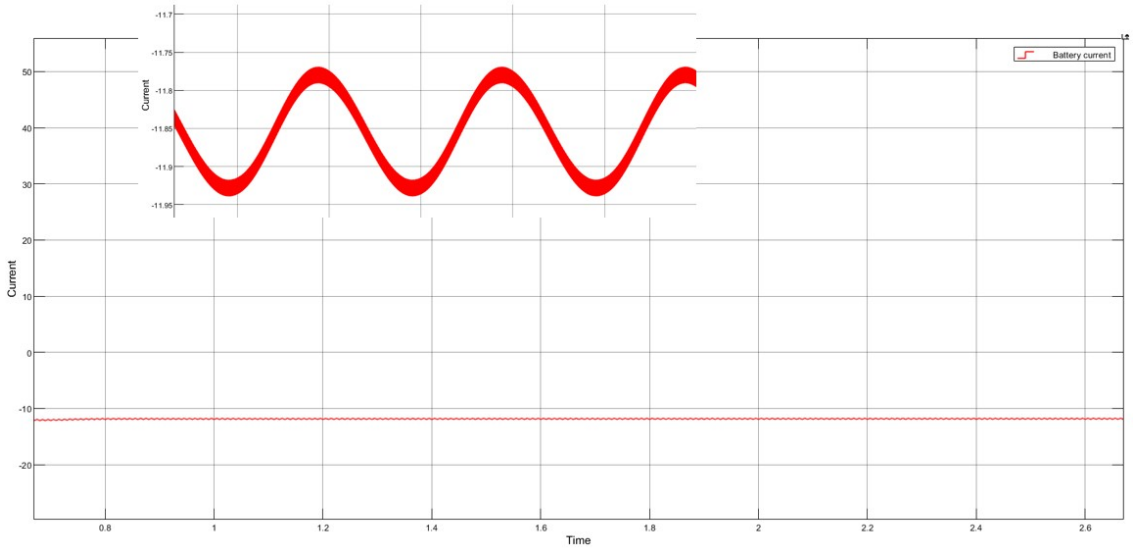

Fig. 3.27: Battery current

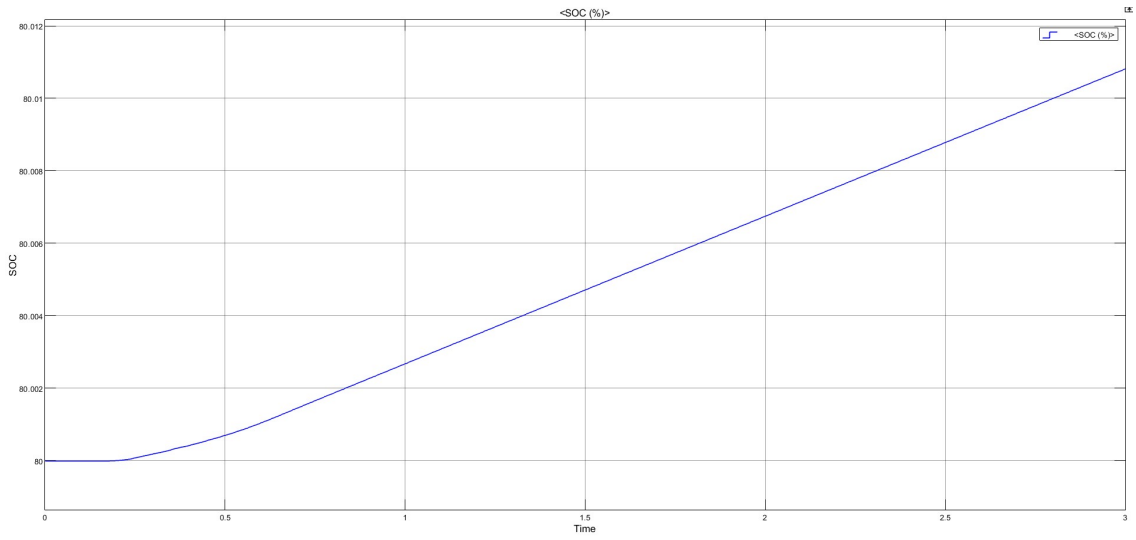

Fig. 3.28: SOC of the battery

Chapter 4

Charging with renewable sources of energy

The source for conventional charging is the ac grid. While normal charging uses the ac grid, which shifts the energy demand from oil to electricity, EVs are an effective way of reducing instantaneous emissions. This ultimately puts further strain on the grid system, which is already dealing with an energy shortage. Nearly 61% of India's electricity is generated by thermal power plants, 15% by hydropower, 8% by solar photovoltaics, 5% by wind energy, 9% by natural gas, and 2% by nuclear power. India is a country with plenty of sunlight, which makes it perfect for using solar energy to generate electricity. PV integration has a bigger impact on the amount of electricity generation as well as power demand reduction, since electricity accounts for the majority of our energy needs. Solar PV systems are flexible stand-alone systems with battery backup, and even though renewables like solar are climate dependent and the Indian climate changes with geography, they are indispensable for remote cities due to their reliability. Additionally, incorporating solar PV with charging stations can assist us in achieving power independence, improving the way we produce electricity, and protecting the land and marine ecosystem from the exploitation of coal and crude oil. The Indian government has a goal of producing 100 GW of solar energy. Three charging levels can be integrated with PV,

but we can't entirely bypass the grid at level 3. Home charging, opportunity charging, and destination charging are three categories of charging. So the standalone PV-battery system can be used in three charging if it's level 1 or 2.

4.1 PV-battery in level 1

With the use of PV and batteries, the grid can be avoided during Level 1 charging or home charging. Here, there are two possible approaches. The first method entails giving PV exclusively to EVs, while the second method entails producing PV for the entire house, as shown in Fig. 4.1. The second approach is

Fig. 4.1: PV integration in home

preferable. If an EV is considered with below specifications

Range of EV – 358 miles The battery capacity of EV – 73.5 KWh

Let it travels a Daily distance – 50 miles

Irradiance duration – 5 hr/ day

From there it's easy to find, KWh/mile=73.5/358= 0.2053 kWh/mile

Total kWh/day = 50 x 0.2053= 10.3 KWh/day

SOLAR PANEL DESIGN:

Solar power needed = 10.3/5= 2.1 KW

Consider Loss= 20%

Net power required= 2.5 KW

Then the needed No of solar panels is approximately equal to 8 panels(325watts)

BATTERY DESIGN:

Specification – 12 V, 250 Ah

Power- 3 KW

Required power= 20 KW

No. of battery = 8

The battery of the above specification can stand with PV to provide the charging.

4.2 PV-battery in level 2

Level 2 charging is a medium charge that requires 4 to 8 hours to complete. When opportunity and destination charging are taken into account, level 2 PV integrated charging can be utilized successfully. For instance, if we need to wait longer than three hours in a theatre, shopping center, school, or college, we have the possibility to charge our electric vehicle. We may charge our vehicles without setting aside any additional time if a standalone PV battery system is installed in the parking lot. More importantly, we can lower the demand for grid power.

Fig.4.3 illustrates the concept of using PV as the parking stand's roof to charge two automobiles simultaneously.Fig.4.2 is a typical level 2 charger; in this case, the power comes from the grid and a battery serves as a backup. So without a grid, this can be converted to PV and batteries.

4.2.1 Design and cost of PV and Battery

We must first take into account the irradiance of the area where the system will be installed. Fig.4.4 displays the solar monthly irradiance and daily irradiance in Kerala, it is clear that there are roughly 5 hours of daylight each day. Consider that 60 KWh per day is required; in this case, it is assumed to be a continuous load

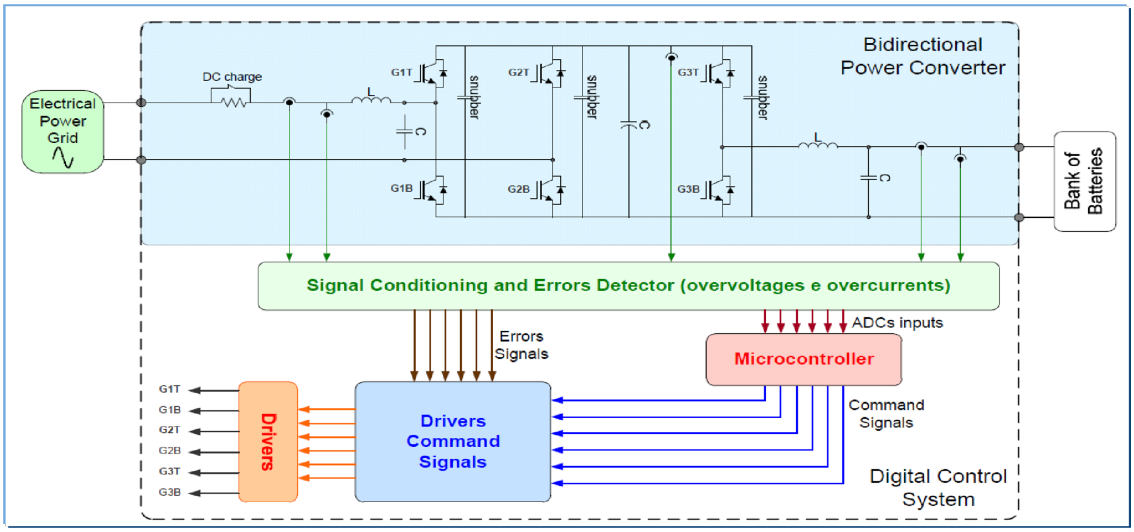

Fig. 4.2: Conventional level 2 charging

of 2.5 kWh per hour, and the system voltage is 240 V (200–250 V). The system is set up as a carport structure in a parking area, with an array serving as the roof and a battery bank nearby. The majority of carport structure manufacturers only permit a 5 to 10-degree tilt; however, a south-facing roof with a 10-degree tilt has been chosen to include a charging station. The available space solely determines the azimuth angle of the solar array. According to IEC Standard level 2, it is designed. The battery bank, charge controller, and PV module are crucial components of this system. The system's operation is simple. During the day, if there is irradiance, PV supplies the load and also charges the battery. The battery powers the load during periods of lower or no irradiance (night time).

Lithium-ion batteries are taken into account in this case, with nominal voltages of 25.6V and 180Ah(C10). The life is assumed to be five years, and the depth of discharge is assumed to be (DOD) 95%.

Consider,Days of autonomy = 2 days.

Battery bank capacity in Ah=U*D*1000/DOD*VSYS= 576Ah

Battery bank capacity in KWH=576*240/1000= 138.24KWh

Total no of batteries required =B*1000/V nom*C1= 30nos

Battery in series=240/25.6= 10nos

Battery in parallel=30/10= 3nos

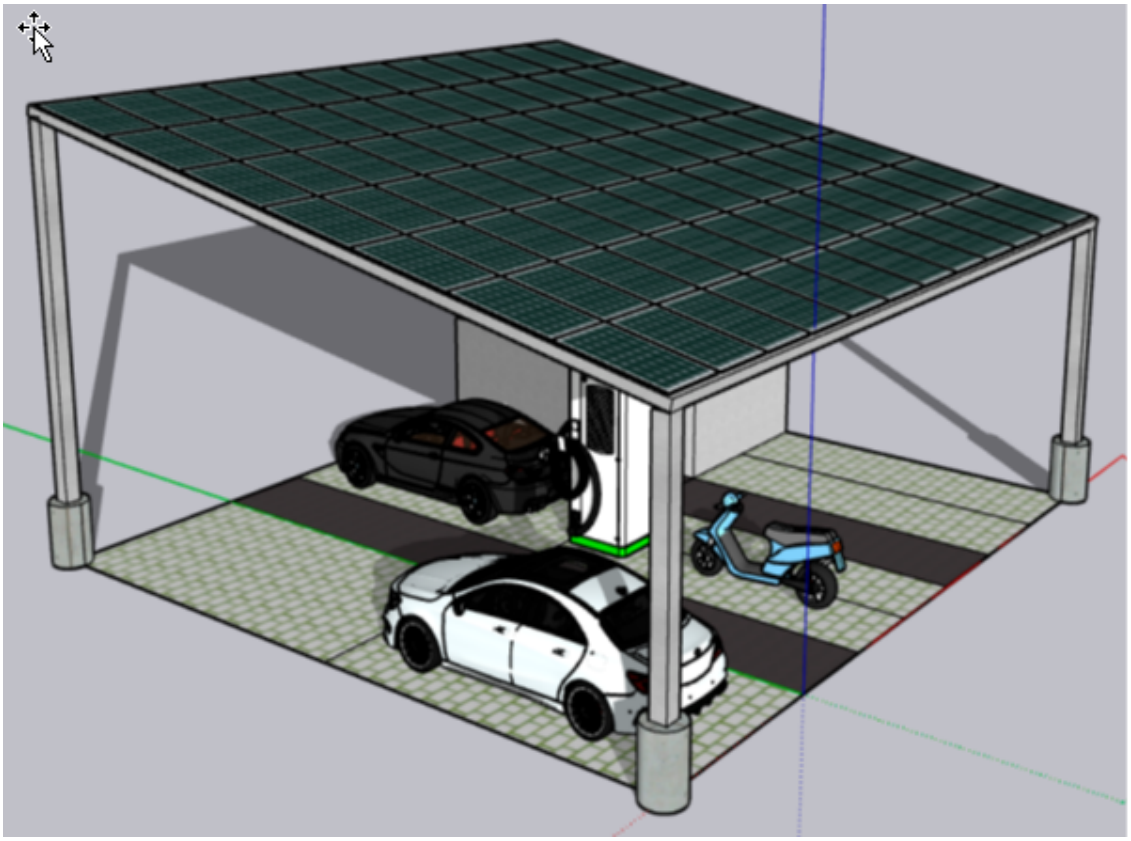

Fig. 4.3: Carport structure

Solar array capacity(KWh)=138.24/0.98= 141.06KWh

Array capacity(KW)=141.06/5= 28KW

So we need to generate 142 KWh from solar

A single 400W Panel can give 1.2-3KWh(average=2KWh)

Total No of panels required = 71 panels

No of panels in series,N_s= V_{sys}/V_{mpp}

No of panels in parallel,N_p= I_{sys}/I_{mpp}

Where Vmpp and Impp are voltage and current at the MPPT point.

When we considered a conventional level 2 charger an approximate cost can be get if it's taken like this,

Machine cost-7-50 Lakhs

Indoor transformer-6 Lakhs(LT)

Electrification-2-3 Lakhs

Total=min of 20 Lakhs

The machines range in power from 25 kW to 340 kW or more. Other varieties

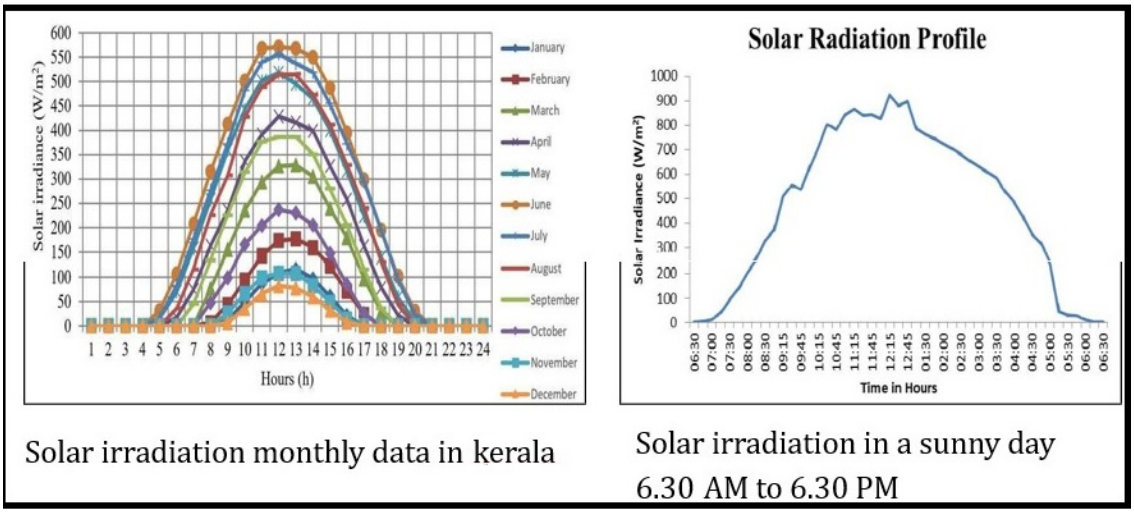

Fig. 4.4: Irradiance profile

start at 30 KW and go up from there. The price ranges from 7 to 50 Lakhs. The electrical board will use nearby transformers to supply power for just one EV under the existing circumstances. It costs about Rs. 6 Lakhs to provide a charging station because the consumer must install the indoor transformers.

For the PV-integrated charging station, the main cost comes from PV and battery bank.

PV cost= 8Lakhs (400W panel- 10,800 to Rs. 13,200)

Battery=76800*30= 23Lakhs(76800 for one battery of above specification)

Machine cost-7-50 Lakhs

Total= min of 40 Lakhs

In order to fully charge a car, around 26 units are required. if we can charge an amount between rupees 20-25 for a single unit, then we get a minimum of Rupees 520 from a single car.

4.2.2 P&O MPPT

Fig.4.5 shows the power, current, and voltage profile with different irradiance for a 200W solar panel. The panel specifications are,

Open circuit voltage=36.3V

Short circuit current=7.84A

Voltage at MPP= 29V

Current at MPP= 7.35A

Fig.4.5 only shows when one series string is taken, we can take the no of series strings and parallel strings according to our bus voltage and current. From the fig it's quite understandable that for every irradiance there is a maximum power point and it needs to be tracked. The method to track MPP is called Maximum Power Point Tracking(MPPT). The indirect approaches and direct procedures are the two main groups of MPPT techniques. The fixed voltage, open circuit voltage, and short circuit current approaches are examples of indirect techniques. Simple presumptions and periodic MPPT estimation are made with simple measurements in this type of tracking. Direct MPPT methods are faster and more accurate than indirect methods since they directly measure the current, voltage, or power. One of the direct MPPT techniques is perturb and observe (P&O).

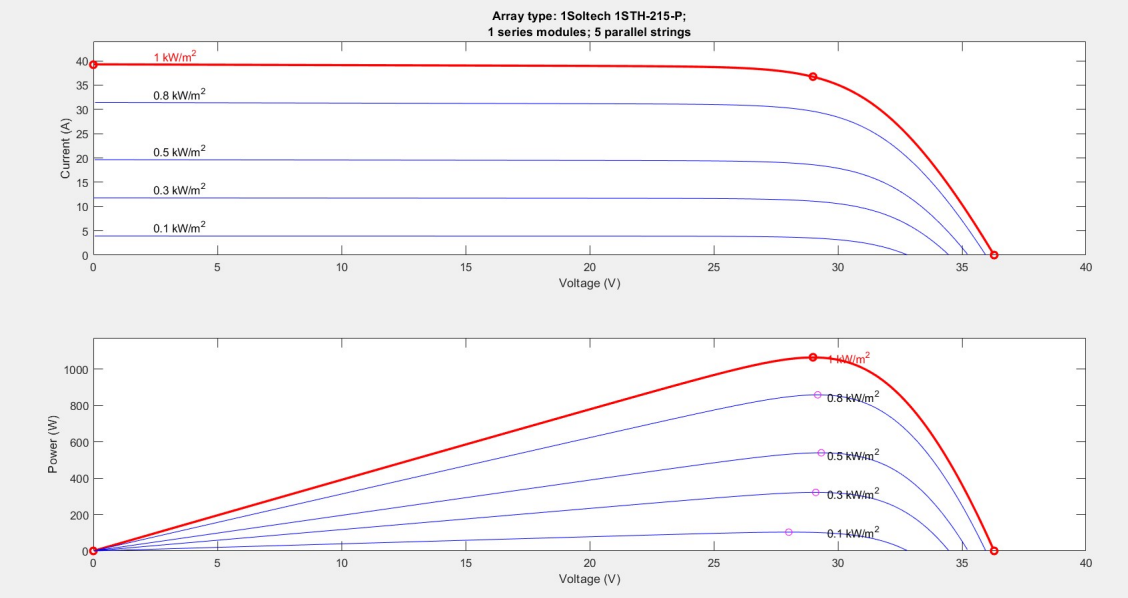

Fig. 4.5: PV power and voltage profile with different irradiance

The P&O MPPT is used to track the MPP. It's done by tracking both the power and voltage. The irradiance curve is shown in Fig. 4.5. From there it's clear that there is a maximum power point at a certain voltage and beyond that the power decreases. So, if the current value of power and voltage is compared with a previous value of power and voltage, the change in power and voltage can be

obtained. With these two values, we can consider different conditions like, change in power and voltage is positive, change in power is positive but the change in voltage is negative, change in power is negative but voltage change is positive, and both voltage and power change is negative. According to the change in power and voltage values, we can track the point and provide a duty cycle corresponding to its position. For example, if the change in power is negative and the change in voltage is also negative that means its shifts to the left of the Power-Voltage profile, so a certain duty cycle value is given to attain the MPP. This duty cycle varies according to the position and provides the MPP. This is the basic working of P&O MPPT. Fig. 4.6 shows the flowchart of the chosen P&O algorithm.

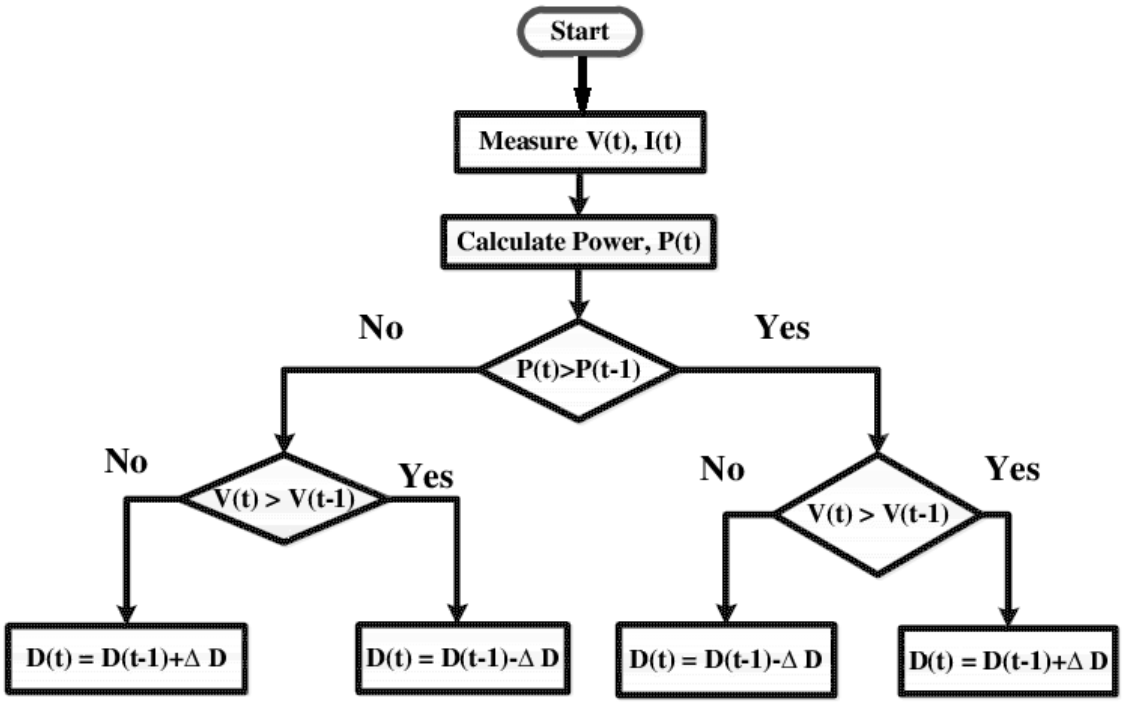

Fig. 4.6: P&O Algorithm

4.2.3 Fuzzy Logic Controller MPPT

To track the maximum power point in photovoltaics, fuzzy logic controllers can be successfully used. The block diagram of an FLC is shown in Fig.4.7. Error (E) and error change (CE) are the FLC's two inputs. The instantaneous panel power and voltage, respectively, are denoted by P(k) and V(k). When looking at the PV characteristics, E decides where the operating point is located, whether it is to the left or right of the peak point, and CE decides how it will move. The output of FLC is the duty ratio, which is provided as a pulse to the boost switch with the help of a PWM generator. The flow chart of FLC MPPT is shown in Fig. 4.9. Here the rule base is created according to the five membership functions which are NB, NS, ZE, PS, and PB.

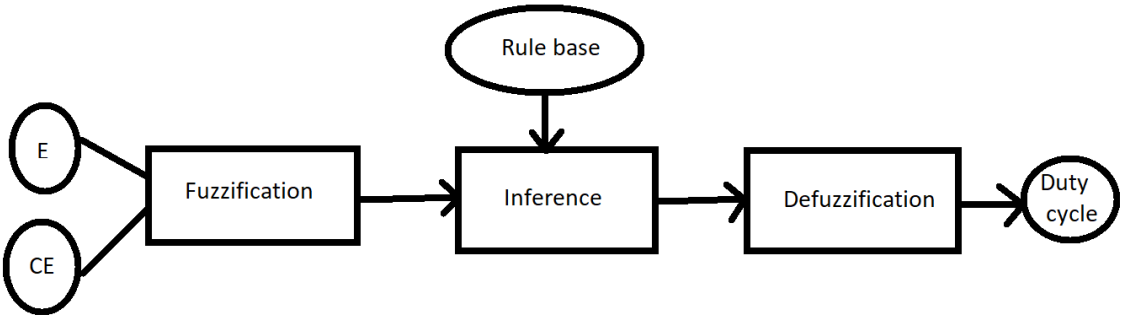

Fig. 4.7: FLC block diagram

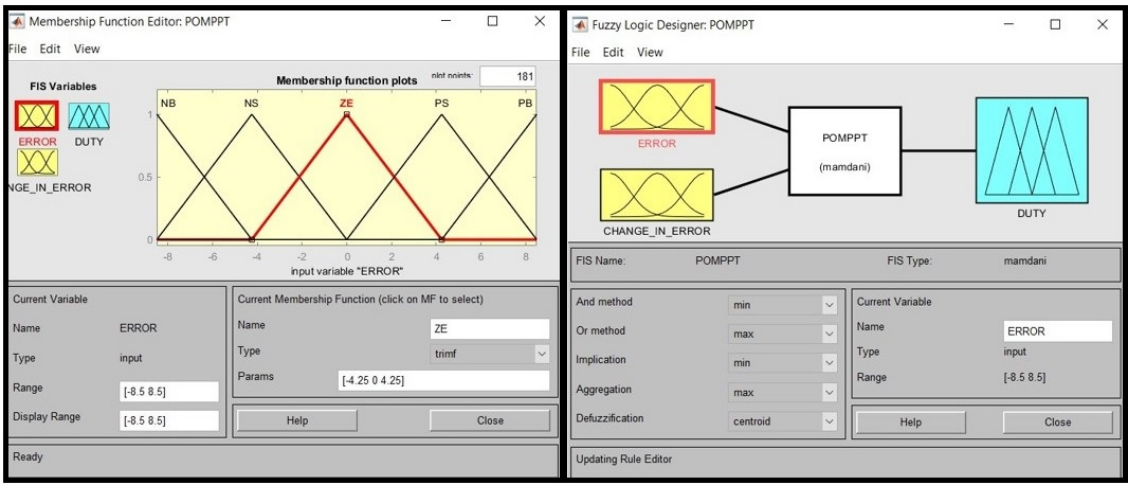

Fig. 4.8: Fuzzy inputs and membership functions

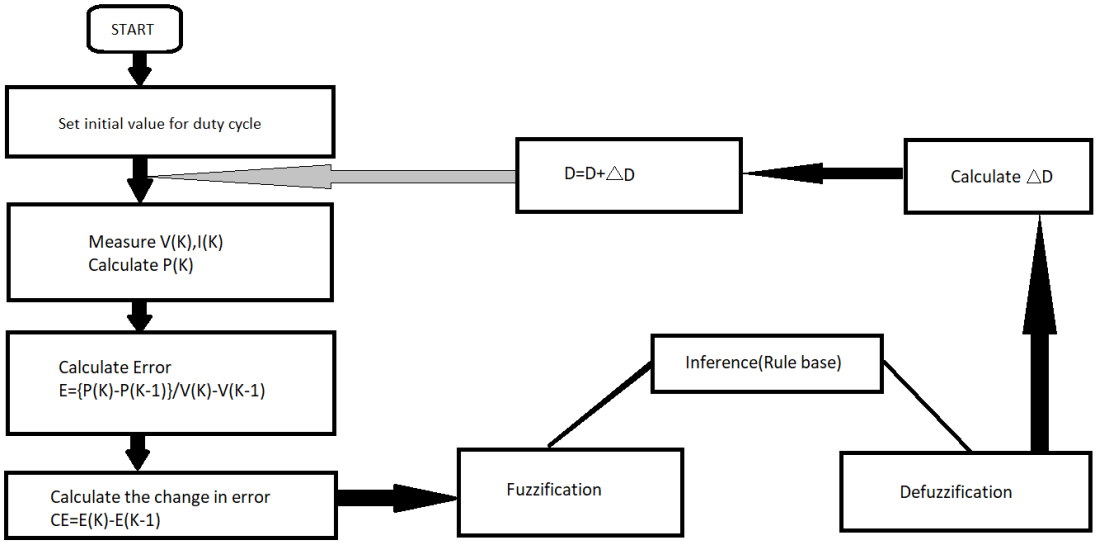

Fig. 4.9: FLC flowchart

4.2.4 Boost design

Here the PV is connected to the boost converter and then to the bus. The boost converter boosts the PV voltage and provides it to the DC bus. The duty cycle of the boost converter can be calculated from the equation below,

$$D = 1 - \frac{V_m \eta}{V_o} \tag{4.1}$$

where V_m is the minimum input voltage, here it's the minimum voltage given by the PV. η is the efficiency and V_o is the output voltage. Here the output voltage is bus voltage.

$$I_i = I_r I_o \frac{V_o}{V_m} \tag{4.2}$$

I_i is the input current, I_o is the output current and I_r is the ripple current which should be considered in between 20% to 40% of the output current.

$$L = \frac{V_m(V_o - V_m)}{I_i f_s V_o} \tag{4.3}$$

L is the inductor value of the boost and f_s is the switching frequency.

$$C = \frac{I_o D}{f_s \Delta V_o} \tag{4.4}$$

Where C is the capacitor value of the boost converter and ΔV_o is the output voltage ripple.

CE / E	NB	NS	ZE	PS	PB
NB	PS	PB	NB	NB	NS
NS	PS	PS	NS	NS	NS
ZE	ZE	ZE	ZE	ZE	ZE
PS	NS	NS	PS	PS	PS
PB	NS	NS	PB	PB	PS

Table. 4.10: Fuzzy rule base

4.2.5 Simulation and Results

Here for the simulation consider a PV panel of 200 watts connected to a boost converter and then connected to a dc bus (dc machine). For the simulation, the system voltage is considered as 48 V so the dc bus needs to maintain a voltage of 48V. The battery taken is 24V 50Ah. The battery charging and discharging are controlled by cascaded pi control, one is outer PI for voltage control and the other is inner PI for current control and also helps to maintain 48V at the bus. Here the minimum input voltage is considered as 25V. The efficiency is considered as 0.9. The output voltage ripple is considered as 1% of the output voltage and the inductor current ripple is taken as 40% of the output current. The boost converter parameters are shown in Table.4.1. The MPPT is very necessary for the PV. There are so many methods for that such as P&O, INC, etc. Here firstly the simulation is done using the basic P&O technique, then Fuzzy MPPT to get a flexible and a better maximum power tracking

Fig. 4.11 shows a simulation of standard level two charging with an AC grid and a battery. Here, a typical rectifier is used to correct the three-phase AC input before it gets connected to the DC bus, and a 200 V battery is included as a backup. The input voltage, bus voltage, and bus current are shown in Fig. 4.12,4.13,4.14 respectively. The bus voltage is 220V and the current is nearly 50A which is a

Table 4.1: Boost Converter parameters

PARAMETER OF BOOST CONVERTER	**PARAMETER VALUES**
Efficiency	0.9
Duty Cycle	0.53
Switching Frequency	20kHZ
Inductor	0.15 mH
capacitor	0.27mF

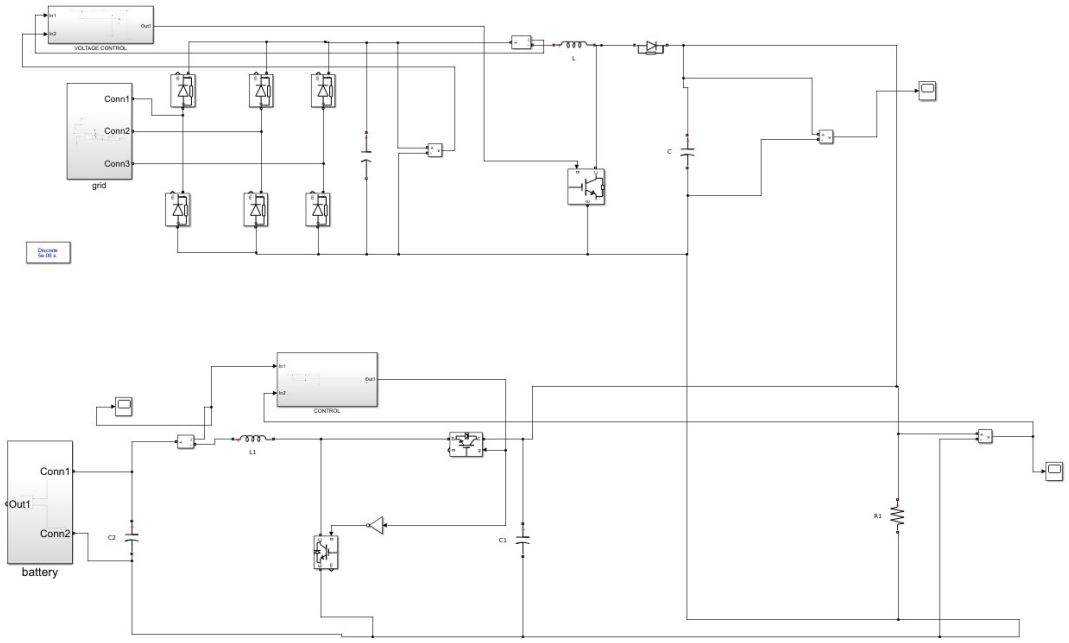

Fig. 4.11: Conventional level 2

second-level changing system specification. The battery powers the load seen in Fig. 4.15 and 4.16 when there is no grid supply.

According to the above-mentioned PV and battery value, the simulation is done which shows in Fig 4.17. By Using a boost converter and P&O MPPT, the PV is connected to the bus. A battery powers the backup, which is managed by a cascaded PI controller. While the inner loop controls current, the outer loop controls voltage. Fig. 4.19 displays the fluctuation in PV voltage and current with respect to various irradiances. PV generates the most power at maximum irradiance, and its output fluctuates with irradiance. The PV-battery response to a change in irradiance is

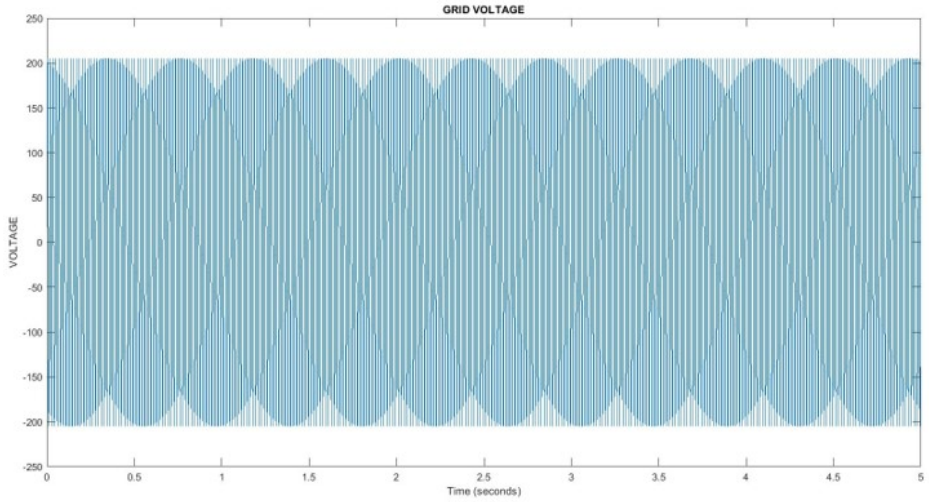

Fig. 4.12: Grid voltage

shown in Fig. 4.20 When there is irradiance, the PV generates power that is, if there is $1000W/m^2$ irradiance, it generates power of almost 1 KW, which also charges the battery. When there is no irradiance or lower irradiance, the PV cannot provide the power so the battery gets discharged and maintain the bus voltage constant with the help of battery control. The fuzzy logic MPPT is employed to achieve better and more flexible power tracking, as seen in Fig 4.18. It is clear from Fig.4.23 that the fuzzy MPPT can deliver a more flexible and stable output compared to P&O MPPT when there is a rapid variation in irradiance.

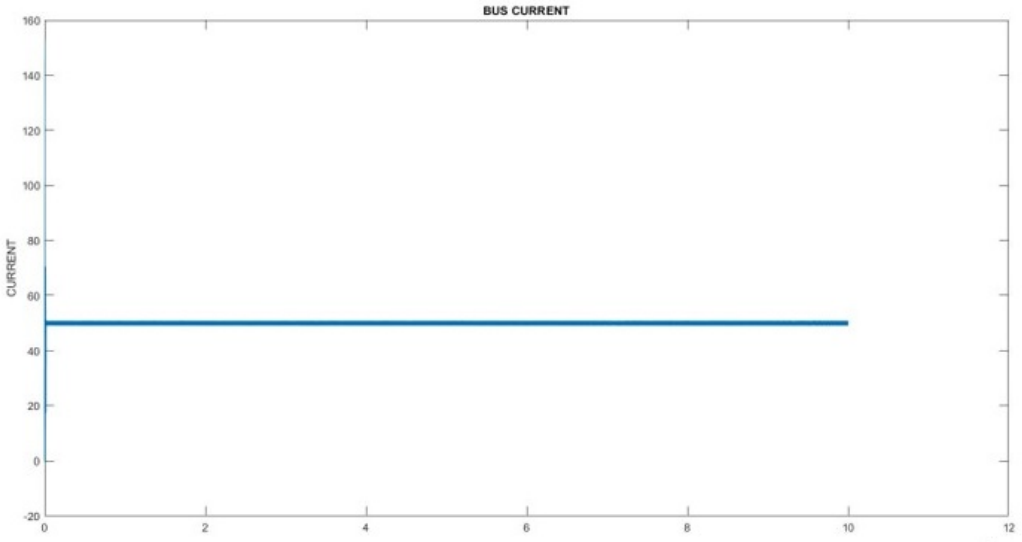

Fig. 4.13: Bus current

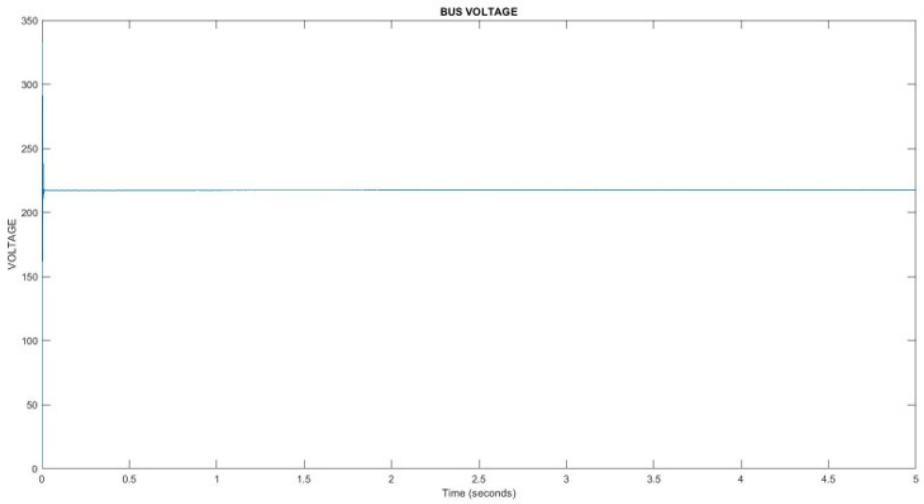

Fig. 4.14: Bus voltage

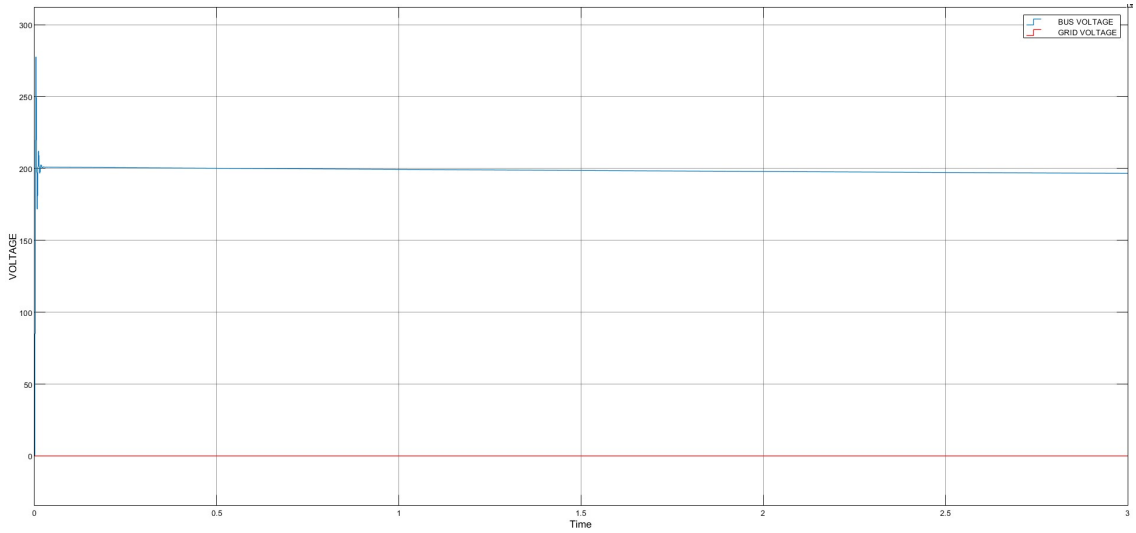

Fig. 4.15: Bus voltage with no grid supply

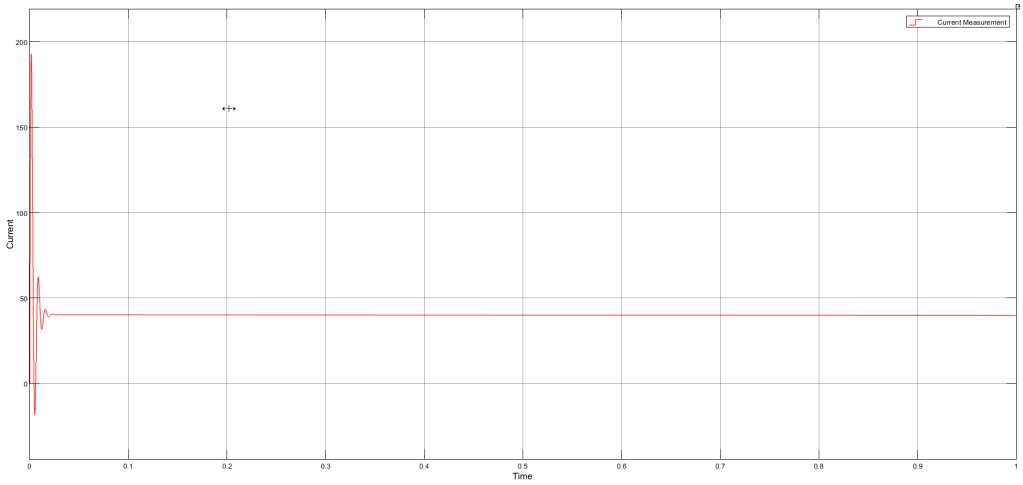

Fig. 4.16: Bus current with no grid supply

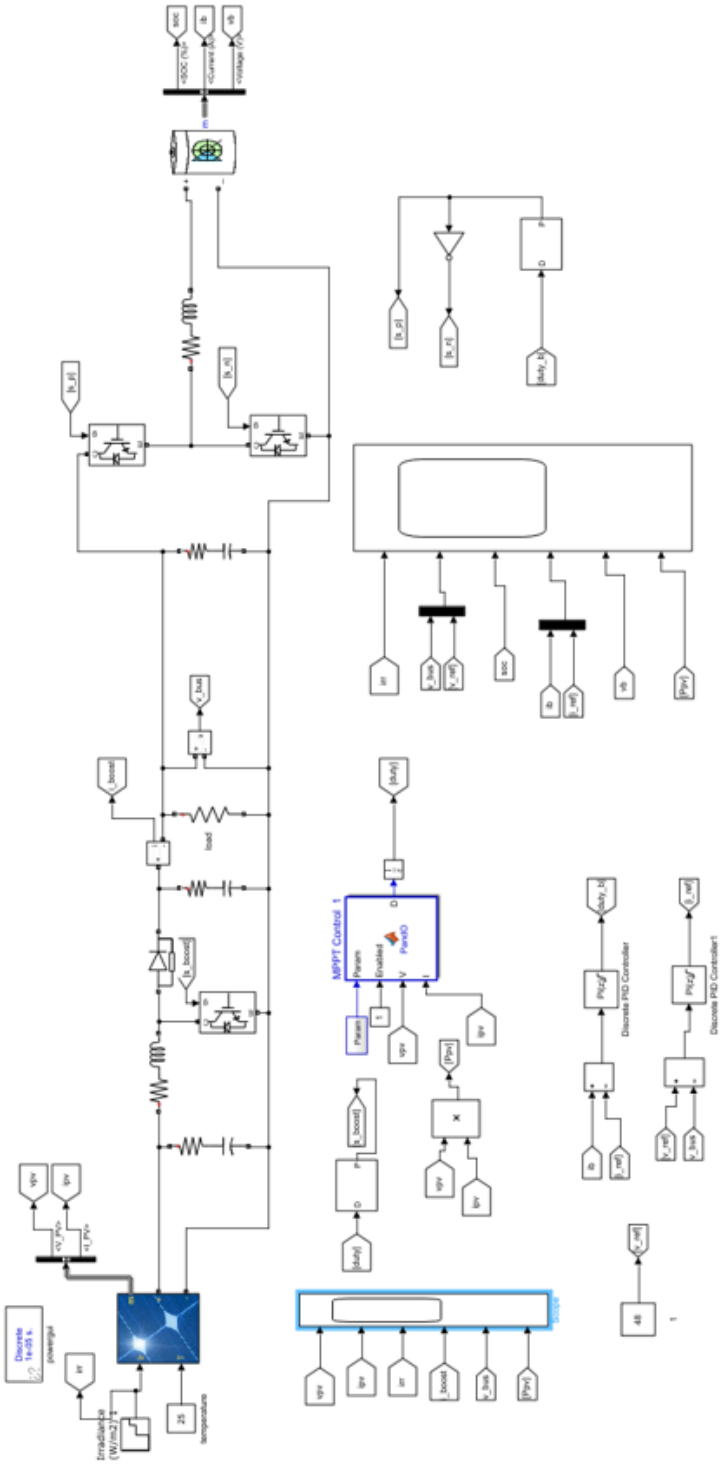

Fig. 4.17: PV-battery with P&O MPPT

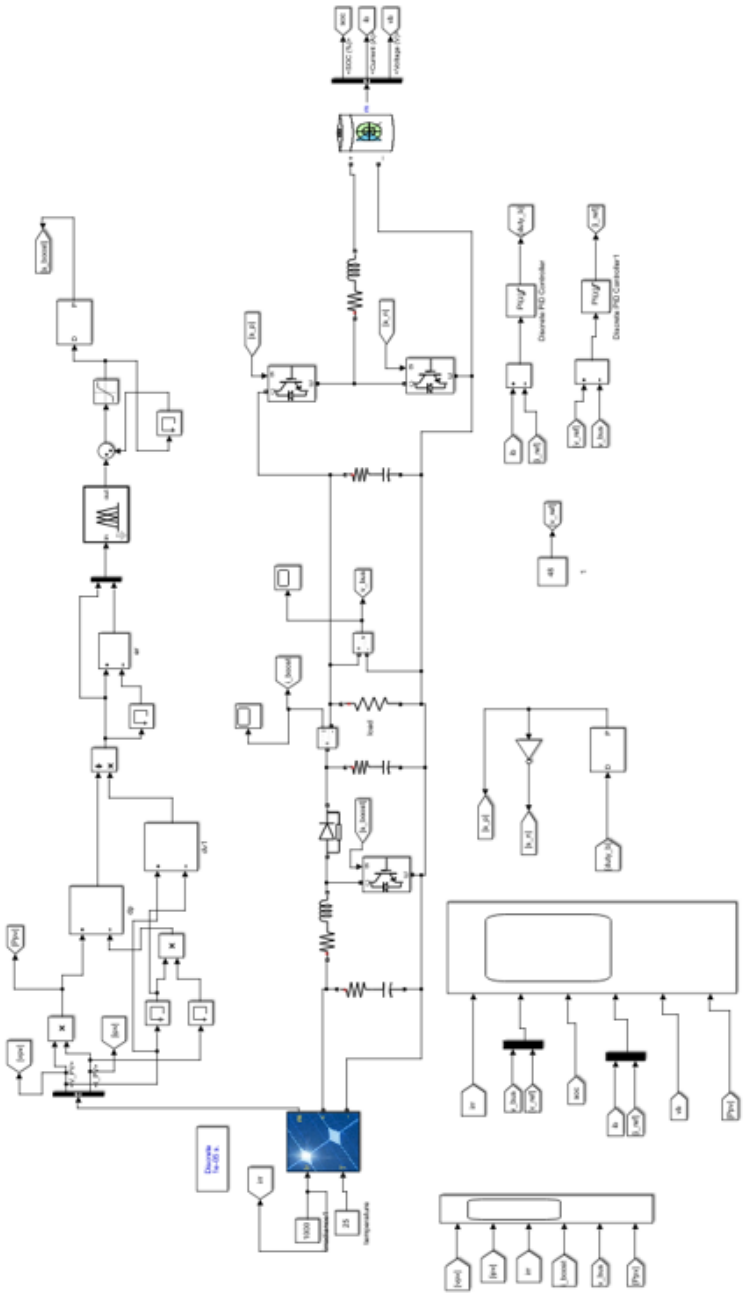

Fig. 4.18: PV-battery with Fuzzy MPPT

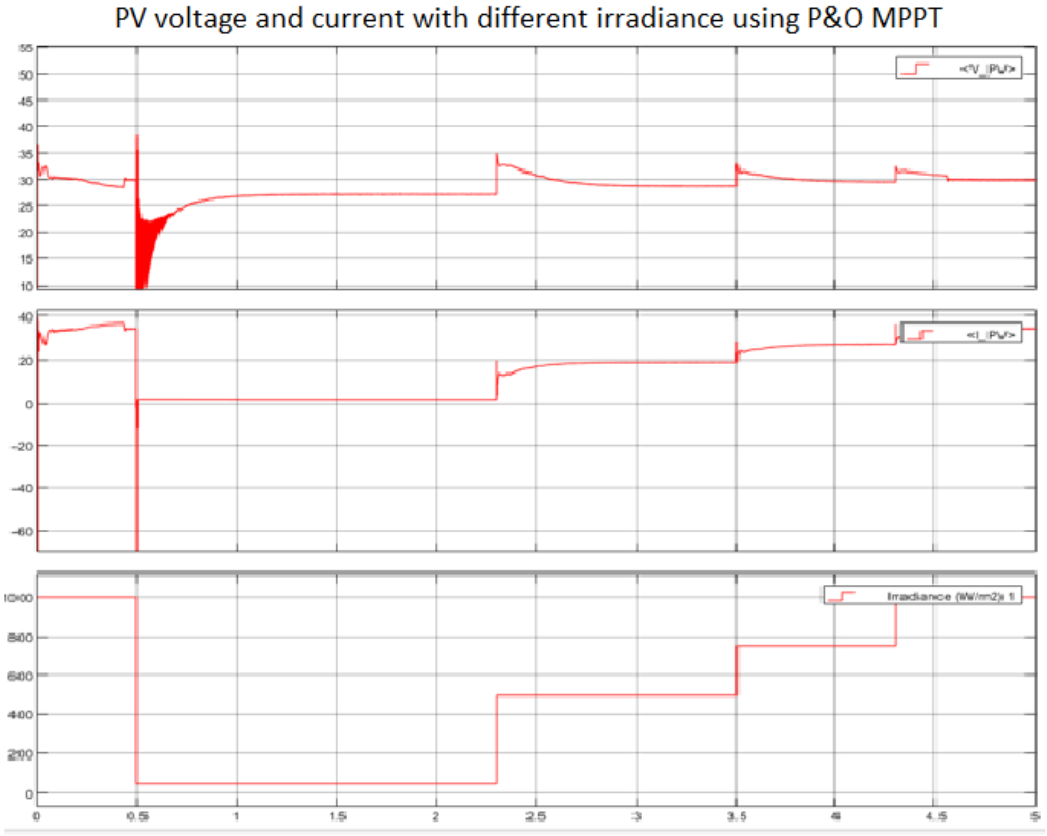

Fig. 4.19: PV-battery response on different irradiance with P&O MPPT

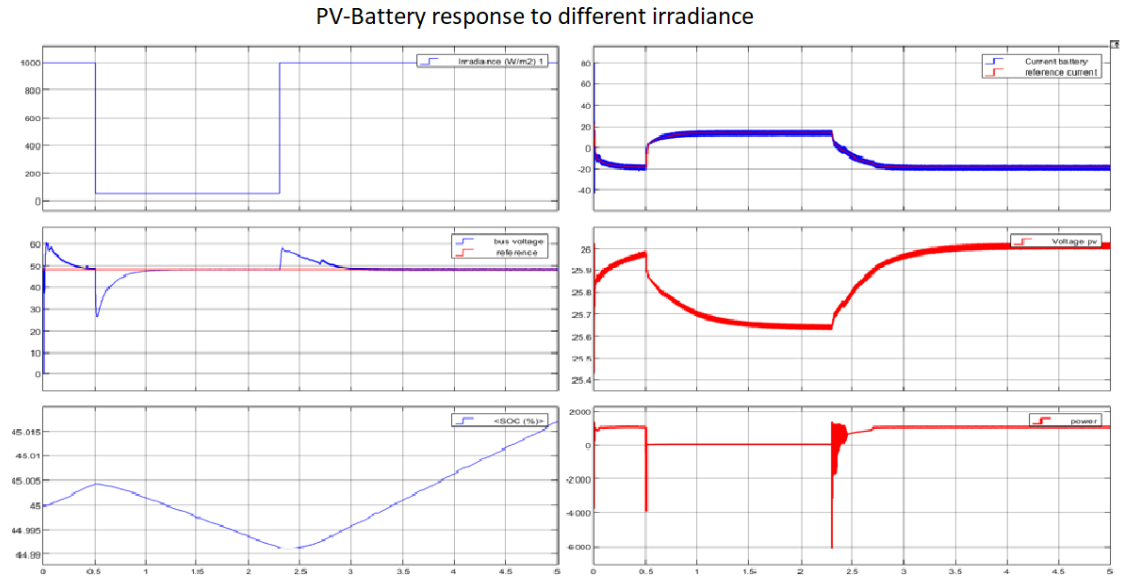

Fig. 4.20: PV-battery response on different irradiance with P&O MPPT

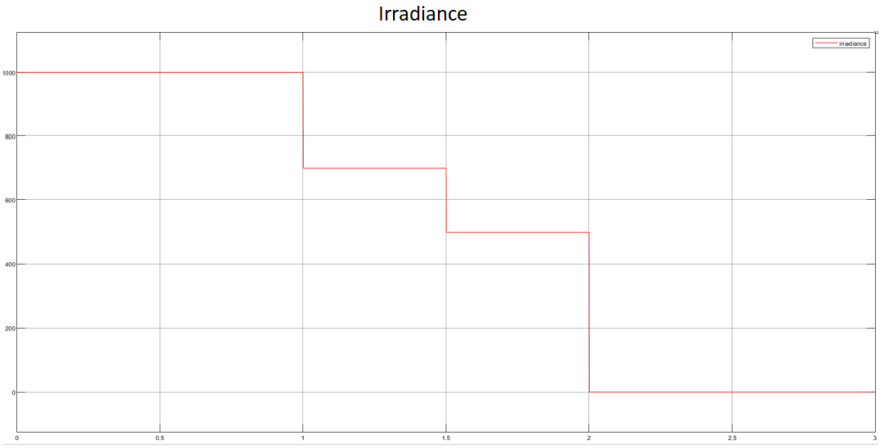

Fig. 4.21: PV irradiance for fuzzy MPPT

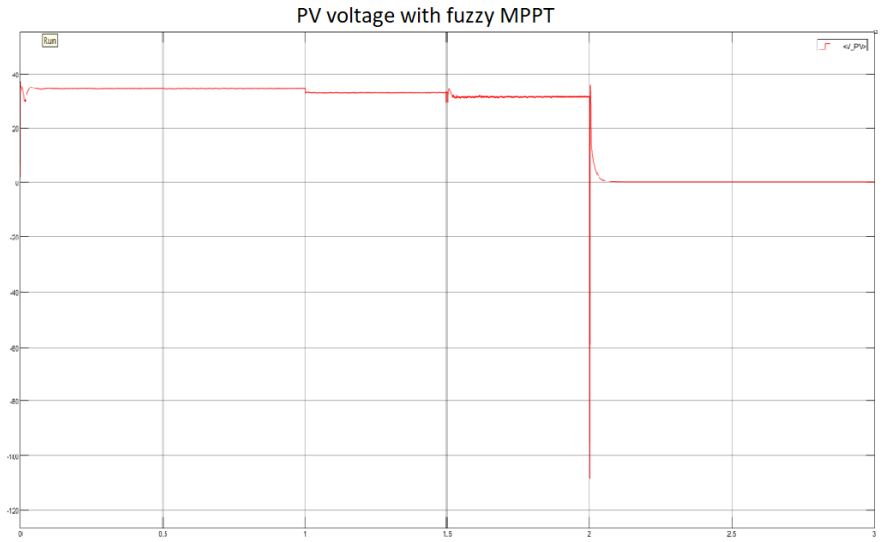

Fig. 4.22: PV voltage when using fuzzy MPPT

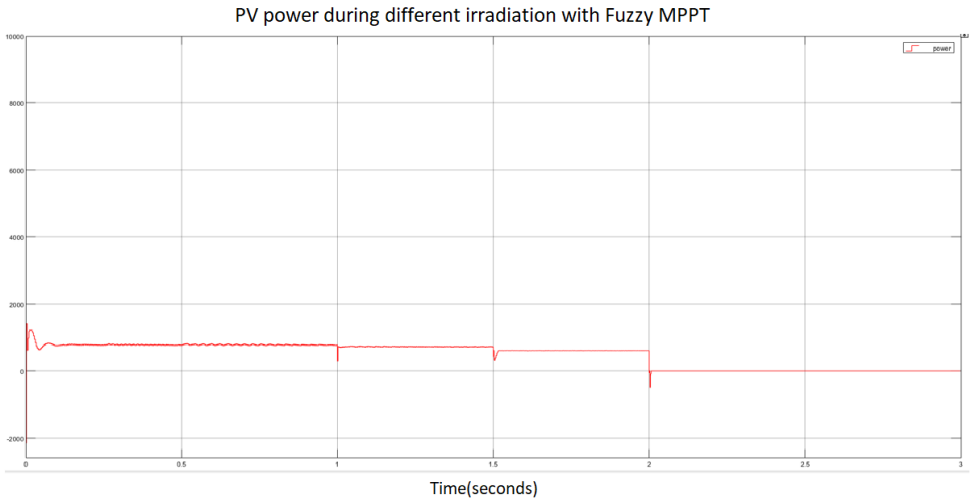

Fig. 4.23: PV power when using fuzzy MPPT

Chapter 5

Future Scope

Another approach to reducing the effect of EV charging on the grid is indirect power demand reduction. In PEVs, the battery is typically powered by a plug-in external source. An EV can produce its own power if a PV panel is installed in it. Let's say an electric vehicle has a 400W solar panel and performs 4.7 miles per KWH on average. A 400W solar panel can generate an average of 2KWH. Then that EV can travel a distance of (2*4.7) 9.4 miles/day. It may cover almost twice as much ground during the summer (almost 19 miles per day). If a 3KWH battery pack is offered as a backup, it helps to go 14.1 miles each day. Therefore, if we have a 400W panel and a 3KWH battery bank, an electric vehicle can travel approximately 23 miles per day.

This approach is adaptable because flexible solar panels are available that can be

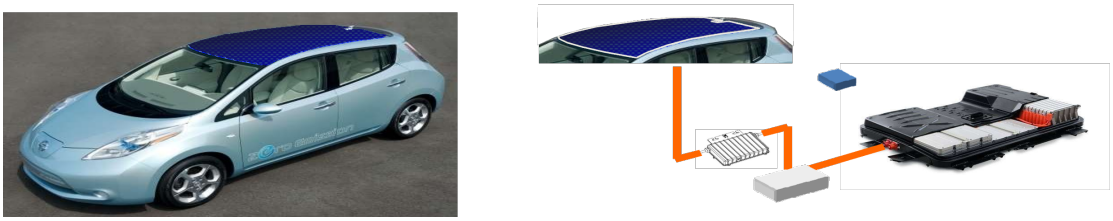

Fig. 5.1: Indirect method

attached to various EV components without affecting their structural features. The

Fig. 5.2: Flexible solar panel

issue here is that we must figure out a way to connect the power produced by the PV directly to the primary or auxiliary battery of the EV.

Chapter 6

Conclusions

Power demand reduction strategies for Level 1 and Level 2 have been analyzed. PFC is one of the crucial ways to lower the excess demand on the grid in level 1 EV chargers. BL isolated Cuk-SEPIC converter with fuzzy logic control has been designed and simulated in DCM for level 1 charger and compared the power factor with Cuk-dc-dc converter topologies(Cuk-flyback, Cuk-push pull). The Cuk-SEPIC topology used here is a single-stage topology and has a lesser no of components than the Cuk topologies which are multi-stage topologies. The charger's cost and size are also decreased, and more crucially, it offers a better PF that is almost equal to unity, which lowers the additional demand on the grid. Another strategy for reducing power demand has been studied by taking into account the implementation design and cost, namely the integration of PV in level 2 charging. It's the ideal approach to entirely avoid the grid and lower the power demand for destination or opportunity charging. It is simulated using fuzzy MPPT and P&O MPPT. A better and more adaptable reaction during a sudden change in irradiance is offered by the fuzzy MPPT.

Bibliography

[1] Aanya Singh, Shubham Sanjay Shaha, and Nikhil P G, *"Design and Analysis of a Solar-Powered Electric Vehicle Charging Station for Indian Cities",* MDPI,25 August 2021, World Electr.Veh.J. 2021, 12, 132.

[2] Dominic Savio Abraham, Rajesh Verma, and, Lakshmikhandan Kanagaraj, *"Electric Vehicles Charging Stations' Architectures, Criteria, Power Converters, and Control Strategies in Microgrids"*, MDPI,6 August 2021, Electronics 2021, 10, 1895

[3] B. Singh and R. Kushwaha, *"A PFC based EV battery charger using a bridgeless isolated SEPIC converter",* IEEE Transactions Power Electronics, vol. 56, no. 1, pp. 477–487, Jan./Feb. 2020

[4] Radha Kushwaha, and Bhim Singh, *"A Power Quality Improved EV Charger with Bridgeless Cuk Converter",*IEEE Transactions Power Electronics, DOI 10.1109/TIA.2019.2918482, IEEE.

[5] D. H. Kim, M. J. Kim, and B. K. Lee, *"An integrated battery charger with high power density and efficiency for electric vehicles",* IEEE Trans. Power Electron., vol. 32, no. 6, pp. 4553- 4565, June 2017.

[6] S. Lee, W. Cha and B. Kwon, *"High-Efficiency Soft-Switching AC–DC Converter With Single-Power-Conversion Method",* IEEE Transactions Industrial Electronics, vol. 64, no. 6, pp. 4483-4490, June 2017.

[7] Murat Yilmaz, and Philip T. Krein, *"Review of Battery Charger Topologies, Charging Power Levels, and Infrastructure for Plug-In Electric and Hybrid Vehicles",* IEEE Transaction on power electronics, VOL. 28, NO. 5, MAY 2013.

[8] M. Mahdavi and H. Farzanehfard, *"Bridgeless SEPIC PFC rectifier with reduced components and conduction losses",*IEEE Transactions Industrial Electronics, vol. 58, no. 9, pp. 4153-4160, Sept. 2011.